The application of RuO_2-based pH-sensors in common beverages

Master thesis

Student:
Iuliia Vetik

Supervisors:
Maryna Lazouskaya, MSc
Department of Chemistry and Biotechnology
Center of Food and Fermentation Technologies

Professor Ott Scheler, PhD
Department of Chemistry and Biotechnology

Study program:
Applied Chemistry and Biotechnology

Tallinn 2021

RuO_2 põhinevate pH-sensorite kasutamine tavalistes jookides

Magistritöö

Üliõpilane:
Iuliia Vetik

Juhendajad:
Maryna Lazouskaya, MSc
Keemia ja biotehnoloogia instituut
Toidu- ja Fermentatsiooni tehnoloogia Arenduskeskus

Professor Ott Scheler, PhD
Keemia ja biotehnoloogia instituut

Õppekava:
Rakenduskeemia ja biotehnoloogia

Tallinn 2021

Autorideklaratsioon

Kinnitan, et olen koostanud antud lõputöö iseseisvalt ning seda ei ole kellegi teise poolt varem kaitsmisele esitatud. Kõik töö koostamisel kasutatud teiste autorite tööd, olulised seisukohad, kirjandusallikatest ja mujalt pärinevad andmed on töös viidatud.

Autor:

Töö vastab bakalaureusetööle/magistritööle esitatavatele nõuetele.
Juhendaja:

Töö on lubatud kaitsmisele.
Kaitsmiskomisjoni esimees:

Contents

Abbreviations

CGE – Conventional Glass Electrode

ED – Electrodeposition

IE – Indicator Electrode

IrOx - Iridium Oxide

IUPAC – International Union of Pure and Applied Chemistry

LD$_{50}$ – Lethal Dose, the average dose of the compound that causes the death of half of the members of the test group.

MOx – Metal Oxide

MS – Magnetron Sputtering

Nafion – Nafion^{TM}

OMC – Ordered Mesoporous Carbon

PVDF - Polyvinylidene Fluoride

RE – Reference Electrode

Introduction

pH is one of the essential parameters in water and food quality control. The pH value influences many chemical and biological reactions during food processing and fermentation processes. The common potentiometric method that is embodied in pH meters is an inexpensive, easy, and fast way of pH measurement. Nevertheless, in many food-processing operations pH control is still carried out offline (Figure 1). The conventional glass electrode (CGE) is not suitable for inline use: its fragility can result in contamination of water or food with dangerous glass fragments.

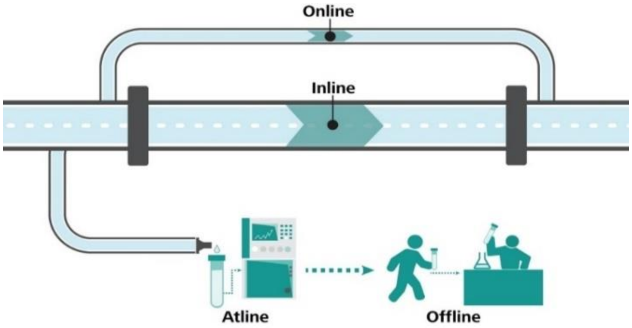

Figure 1. A measuring device can be applied to an industrial line in the following ways: (i) inline – when the entire flow is evaluated; (ii) online – when some amount of the flow is directed to a small tube with a build-in measuring device and (iii); offline – when a small amount of the flow is directed toward a faucet allowing to collect a sample for further investigating by a researcher or a machine (atline) (reproduced from [1]). At present, offline pH measurement is the dominant way to measure pH.

The modern alternatives to the CGE are proton sensitive all-solid-state metal oxide sensors, among which ruthenium dioxide (RuO_2) electrodes are the most promising. RuO_2 electrodes have such advantages as high pH sensitivity, mechanical durability, and low cost. Nevertheless, all ruthenium compounds are considered toxic and cancerogenic. To overcome this problem a partial replacement of RuO_2 by the much less toxic and less expensive copper oxide is proposed in this thesis.

The main objective of this work was to investigate the applicability of RuO_2-based electrodes for pH measurement in beverage samples as an alternative to a conventional glass electrode. Main aims of the work included determining electrochemical characteristics of RuO_2-based electrodes and their performance in real-life aqueous samples. Furthermore, this work aimed to compare the abovementioned parameters to those of CGE.

The thesis consists of 4 parts. 1. Literature overview describes the potentiometric method used for pH measurement, working principles of the CGE and RuO_2 electrode. The main objectives of the study are listed in 2. Aims of the work. Chapter 3. Materials and methods contain the information about used equipment and chemicals and describe the main methods: screen-printing method, that was applied for fabrication of electrodes, and the standard potentiometric method, the pH measurements were performed by. For the convenience of perception of information, 4. Results and discussion have been united into one chapter, that contains both the received data and an explanation of it.

As a result of the current work, the novel binary ruthenium oxide-copper oxide electrodes that have not been investigated and described before were developed. The developed electrodes have electrochemical characteristics similar to that of pure RuO_2 electrodes and a CGE. Furthermore, binary electrodes reported in this work showed better performance in beverage samples compared to that of the pure RuO_2 electrodes.

1. Literature overview

1.1. What is pH

According to the International Union of Pure and Applied Chemistry (IUPAC), pH is one of the most frequently measured physicochemical quantities[2]. The measurement and control of the acidity of a sample are essential in a wide range of processes, including food production and quality control. pH value can be a mark of protein denaturation[3], growth and mortality of microorganisms[4],[5], the germination or inactivation of bacteria spores[6],[3]. High pH values can indicate the poor structure of meat[7] or long storage and therefore spoilage of fish[8]. Increased pH value of milk can indicate inflammatory infection of cows[9].

The concept of pH is unique in the sense that it is based on the quantity of a single ion present in an analyte. IUPAC defines pH in terms of the activity of the hydrogen ions (H^+) in solution as follows[2]:

$$\mathrm{pH} = \mathrm{pa}_{\mathrm{H}^+} = -\,\mathrm{lg}(\mathrm{a}_{\mathrm{H}^+}) = -\mathrm{lg}\left(\frac{\mathrm{m}_{\mathrm{H}^+}\gamma_{\mathrm{m,H}^+}}{\mathrm{m}^{\varnothing}}\right) \tag{1}$$

where *p* is interpreted as an operator ($px = -lgx$), a_{H^+} is the activity of hydrogen ions in an aqueous solution ($H^+_{(aq)}$), γ_{m,H^+} is the activity coefficient of $H^+_{(aq)}$ at molality m_{H^+}., $m^{\varnothing}$ is the standard molality, 1 mol kg^{-1}.

1.2. Potentiometric method of pH determination

IUPAC has developed recommendations for procedures related to pH measurement in dilute aqueous solutions in the temperature range of 5–50°C[10]. According to IUPAC recommendations, routine pH measurement is carried out by the potentiometric method in an electrochemical cell containing a glass electrode serving as a combination of an indicator electrode and a reference electrode. The conventional glass (CGE) electrode is described in section 1.5. The working principle of the conventional glass electrodeCertified buffer solutions should be used for calibration of the glass electrodes used for pH measurement[10].

Potentiometry is a versatile analytical method that allows simple and rapid analysis of various samples[11]. It is based on the measuring of the potential of the electrochemical cell with low current applied[12]. The electrochemical cell for the determination of the activity of H^+ ions consists of (i) a measuring device (e.g., potentiometer), (ii) two electrodes: indicator electrode (IE) and reference electrode (RE), and (iii) electrolyte (analyte solution) through which ions are conducted (Figure 2).

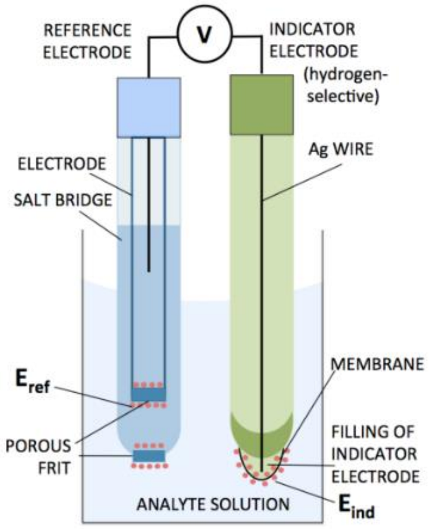

Figure 2. The electrochemical cell for the determination of the activity of H^+ ions consists of a potentiometer (V) and two electrodes: hydrogen-selective indicator electrode (green) and reference electrode (blue), and analyte solution through which ions are conducted (adopted from[13]).

The potential of the potentiometric cell (E_{cell}) is a difference between the potential of IE and RE:

$$E_{cell} = E_{ind} - E_{ref} \tag{2}$$

where, E_{ind} is the electrochemical potential of the reaction taking place on the indicator electrode, V; E_{ref} is the electrochemical potential of the reaction taking place on the reference electrode, V.

In general terms, the redox reaction taking place on the electrode can be represented as follows:

$$A_{ox}^{n+} + ne \rightleftarrows A_{red} \tag{3}$$

where A_{ox} is the oxidized form of the element, A_{red} is the reduced form of the element, and n is the number of electrons or participating in the electrode reaction.

The potential of any electrode (E) depends on the activity of the ions participating in the electrode reaction according to the Nernst equation[12]:

$$E = E^0 + \frac{R \cdot T}{n \cdot F} \cdot \ln \frac{a_{ox}}{a_{red}} \tag{4}$$

where, E^0 is standard electrode potential[1], V; n is the number of electrons or participating in the electrode reaction; R is the universal gas constant (R = 8.314 J/(K·mol)); T is absolute temperature, K; F is Faraday constant (F = 96485°C/mol); a_{ox}, and a_{red} are the activities of the oxidized and reduced forms of the electrode material respectively, mol/L.

After substituting constants, at room temperature (T = 21°C or 294°K) Nernst equation takes the following form:

---

[1] **Standard potential** is a measure of the individual potential of a reversible electrode (in equilibrium) in a standard state (concentration 1 mol l^{-1}, pressure 1 atmosphere and temperature 25 °C).

$$E = E^0 + \frac{0.0584}{n} \cdot lg \frac{a_{ox}}{a_{red}} \tag{5}$$

Therefore, knowing what electrochemical process takes place on the electrode and measuring the potential it is possible to find activities of the ions participating in the process. If hydrogen ions participate in the reaction, it is possible to measure H^+-ions concentration (activity) and therefore the pH value of the solution.

1.3. Indicator electrodes

An indicator electrode is an electrode, the potential of which depends on the activity (concentration) of the detected ion in the analysed solution[12]. There are two groups of indicator electrodes: metallic electrodes and membrane electrodes. For the metallic electrodes, the potential appears as a result of an electrochemical reaction involving the electrode's material (e.g., for a Cu, Ag, Pb[12]). Since the electrochemical reaction taking place involves electrons such electrodes have electronic permeability. For the membrane electrodes, the potential is a result of ion-exchange reaction at the electrode/solution interface, electrodes have ionic permeability[11]. The classification of the working principle of the indicator electrodes is presented in Table 1.

1.4. Reference electrodes

A reference electrode provides a stable potential that is independent of the composition of the analysed solution. A reference electrode must be chemically stable and should not affect the probe. Its potential should not change with the current.

The most suitable ones for being reference electrodes are the electrodes of the second kind[2] (Table 1). For example, a conventional pH probe embodies an Ag/AgCl reference system[14] that consist of an Ag wire, poorly soluble AgCl and a chloride-containing electrolyte solution. The potential of this electrode depends on the concentration of the chloride ions but does not depend on the pH value of the solution[12]. Therefore, the potential of Ag/AgCl electrode stays stable in the solutions with different pH making the electrode suitable to be a reference electrode for pH measurements.

In potentiometric pH measurement, the reference electrode is usually grounded and its potential is considered zero. Therefore, the potential of an electrochemical cell is equal to the potential of the indicator electrode as can be seen from equation (2).

---

[2] **An electrode of the second kind** is an electrode, consisting of a metal covered with a slightly soluble salt of this metal immersed in a solution containing the same anion as the salt[12].

Table 1. Classification of the indicator electrodes[11],[12].

	Electrode type	Description	Examples
Metallic electrodes	The first kind	pure metallic electrodes	$Ag^+|Ag$ $Zn^{2+}|$ Zn
	The second kind	a metal covered with its slightly soluble salt immersed in a solution containing the same anion	$Cl^-|AgCl_{(s)}$,Ag; $Cl^-|Hg_2Cl_{2(s)}$,Hg
	Red/Ox electrodes	inert electronic conductor (e.g. Pt, Pd, Au) immersed in a solution containing a Redox pair of an element	Fe^{3+},$Fe^{2+}|$Pt; MnO_4^-,$MnO_4^{2-}|$Pt
	Metal oxides	a layer of metal oxide (or a mixture of metal oxides) on conductive substrates	$OH^-|$HgO,Hg; $OH^-|Sb_2O_3$,Sb
	Gas electrodes	a Pt wire immersed into a solution of an acid through which gas is flown	$H^+|H_2$,Pt; $Cl_-|Cl^2$,Pt
Ion-selective electrodes	Glass electrode	glassy (non-crystalline) membrane typically based on silicon oxide network that is doped with a relatively high concentration of Li_2O and/or Na_2O	conventional pH glass electrode
	Solid membrane electrodes	a membrane of slightly soluble crystalline material with an ionic conductivity type	membrane based on AgCl membrane based on CuS
	Liquid and polymeric membrane electrodes	traditionally membrane is made from a simple organic highly viscous liquid embedded in a porous matrix, nowadays it is replaced with a polymers	Valinomycin (K^+-selective) membrane Nonactin/Monactin (NH_4^+ selective) membrane
	Ion-exchanger-based electrodes	liquid polymeric membranes that exhibit ion-exchanger properties so that the concentration of analyte in the membrane phase remains approximately constant as the sample concentration is changed	(tridodecylmethylammonium chloride (anion-selective) potassium tetrakis (4-chlorophenyl) borate (cation-selective)
	Gas sensitive electrodes	gas-permeable membrane	microporous Teflon membrane with an inner solution containing bicarbonate salt (CO_2 sensitive)
	Enzyme electrodes	membrane with an incorporated thin layer of enzyme	a biosensor with immobilized urease at an ammonium-selective electrode (urea-selective)

1.5. The working principle of the conventional glass electrode

The glass electrode is one of the ion-selective membrane electrodes. Its potential linearly depends on the logarithm of the activity of hydrogen ions. The electrode has a glass membrane, that is permeable only to H^+ ions. The typical thickness of the membrane is in the range between hundreds of micrometres to one millimetre[11].

A modern glass pH electrode is a combination electrode that integrates indicator and reference elements in the same body (Figure 3a). Generally, both electrodes are metal electrodes, consisting of silver wire covered with silver chloride that is immersed in a solution containing chloride ions (slightly acidic (pH ~6) pH buffer for indicator electrode, and KCl electrolyte for the reference electrode[11]).

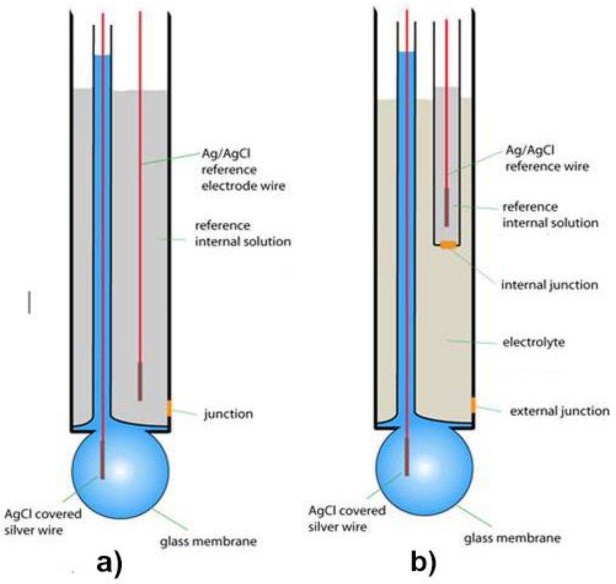

Figure 3. Glass combination electrodes integrate indicator and reference elements in the same body: single-junction electrode **(a)** has a junction that allows contact between the reference system and the sample solution and double junction electrode **(b)** has an additional chamber that prevents contamination of the electrode inner solution with the sample (adopted from [15]).

The combination electrode has a junction that allows contact between the reference system and the sample solution. Under adverse conditions (high temperature, highly acidic conditions etc.), the reference electrode can be contaminated with sample residues due to ingress of sample into the reference compartment[16]. The double junction electrode (Figure 3b) has an additional chamber that prevents contact between the electrode's inner solution and the sample. This way the contamination of the electrode is minimized, leading to a longer electrode's life[17]. Such electrode is the most popular solution for measurement in food samples.

The membrane of the glass electrode has to be soaked in water before the start of a measurement. In contact with water, a gel-like hydrated layer (up to 100 nm[11]) is formed on the surface of the glass (Figure 4). At room temperature, the swelling of the membrane takes up to 24-48 h[14].

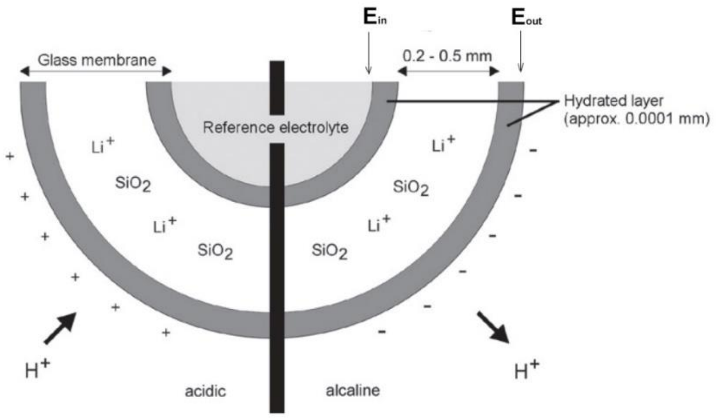

Figure 4. When the glass electrode is placed into an aqueous media, a hydrated layer is formed on the surface of the membrane of the glass electrode. Hydration of the glass membrane is accompanied by an exchange reaction between cations of alkali metal in glass and protons in an aqueous solution. This reaction underlines the pH response of the glass electrode (adopted from [14]).

Hydration of the glass membrane is accompanied by an exchange reaction between alkali metal cations in glass and solution protons. The pH response arises due to this exchange reaction[12]:

$$\mathrm{H^+ + Na^+Glass \rightleftarrows Na^+ + H^+Glass} \tag{6}$$

In the case when H^+ ions activities are different on the different sides of the membrane, the potential arises. This potential is the difference between boundary potentials on both sides of the membrane (Figure 4):

$$E = E_{out} - E_{in} \tag{7}$$

where E is membrane potential, E_{out} and E_{in} are the boundary potentials on the outer and inner sides of the membrane. Since the activity of hydrogen ions in the internal solution of the glass electrode is constant, the potential of such electrode becomes a measure of the activity of hydrogen ions in the external solution[12]. Equation (5) for glass electrode takes the following form:

$$\mathrm{E} = const + 0.0584 \lg \mathrm{a_{H^+}} = const - 0.0584\ \mathrm{pH} \tag{8}$$

The *const* value includes the potentials of the external and internal reference electrodes and depends on the type of glass and temperature[12]. This value changes in the process of electrode exploitation, which is why glass electrode needs regular calibration. The factor before pH is called sensitivity and describes how accurately the electrode works. The value 0.0584 V/pH (or 58.4 mV/pH) is theoretical or Nernstian sensitivity for room temperature.

CGE have close to Nernstian pH response, high accuracy, and selectivity. These electrodes are stable over a wide range of pH values and have a long lifetime. However, glass electrodes have some disadvantages as well. Along with the need for regular calibration, CGEs have a large size, and it is hard to miniaturize them. Corrosive environment, strong acids and bases can influence the stability of electrodes. Moreover, the biggest issue is the mechanical fragility of glass electrodes; pollution with glass shards is dangerous in the food industry.

1.6. Solid-state metal oxide electrodes

A modern alternative to the glass electrode is the pH sensors based on the various metal oxides (MOx) that exchange electric charge at electrode-electrolyte interfaces. MOx electrodes are not only stable mechanically and chemically, but also show good performance in extreme conditions[18]. Such sensors are fit for online monitoring and can be easily miniaturized for flexible systems[19].

The working principle of the MOx based electrodes is similar to the CGE and is based on the selective response to the H^+ ions present in an electrolyte. Trasatti[20] suggested the most probable sensing mechanism[6], according to which pH response arises due to the formation of the hydroxide layer by dissociative adsorption of water. The mechanism will be described in detail in section 1.7.2. Working principle of the ruthenium dioxide pH-electrode In general, the following reaction occurs on the surface of MOx based electrode:

$$\mathrm{Me^{A}O_{x}(OH)_{y} + ne^{-} + nH^{+} \rightleftharpoons Me^{A-n}O_{x-n}(OH)_{y+n}} \qquad (9)$$

The formation of a couple of higher and lower valency MOx lead to the generation of a potential difference between the IE and RE. The value of the potential can be expressed by the Nernst equation:

$$\mathrm{E = E^{0}_{Me^{A}/Me^{A-n}} - \frac{R \cdot T}{n \cdot F} \cdot \ln \frac{a_{Me^{A-n}}}{a_{Me^{A}} \cdot a_{H^{+}}}} \qquad (10)$$

Since metal oxides are in a solid state, the activity of metals approximates 1 (a_{Me}=1), the equation (10) takes the form of:

$$\mathrm{E = E^{0}_{Me^{A}/Me^{A-n}} - \frac{R \cdot T}{n \cdot F} \cdot pH} \qquad (11)$$

Therefore, according to equation (11) the potential of the MOx based electrode is proportional to the pH of the solution.

The sensitivity of MOx electrodes significantly depends on the type of materials and the method used for its fabrication. MOx sensors vary in terms of sensitivity, hysteresis, and drift. Some of the MOx electrodes are undesirably cross-sensitive to several redox agents[6]. This cross-sensitivity leads to limitation of the performance in pH measuring, e.g. for electrodes based on antimony and bismuth[6]. At the same time, some of MOx have very good sensitivity and selectivity to hydrogen ions, and a high degree of accuracy. For example, metal oxides of Pt-group (e.g. RuO_2, IrO_2) that show sensitivity close to the ideal Nernstian response (58.4 mV/pH at 21 °C, see equations (4) and (5)) (Figure 5).

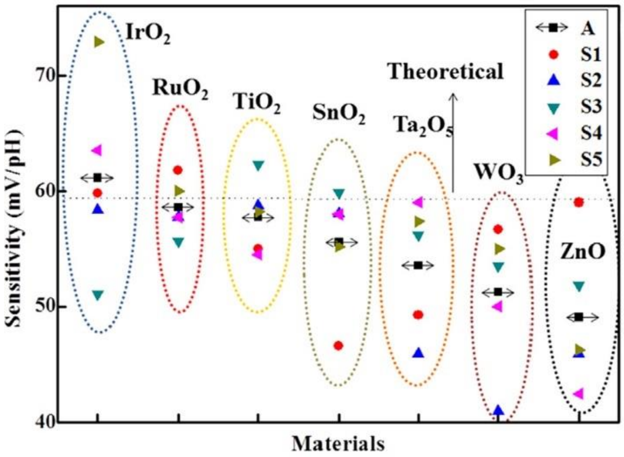

Figure 5. Electrodes based on metal oxides of Pt-group, especially IrO_2 and RuO_2, show the best pH-sensitivity compared to other metal oxides (dash line – theoretical Nernstian sensitivity, A – average sensitivity of group, S1-S5 – sensitivities of samples 1-5). (reproduced from [19]).

1.7. All-solid-state ruthenium dioxide electrode

The ruthenium dioxide (RuO_2) is used in electrochemical sensors, electrocatalysis and supercapacitors[6]. It is a mixed electronic and ionic conductor with a conductivity of 25 000 S cm^{-1} at room temperature[18]. Such a high conductivity in addition to high stability allows electrodes based on RuO_2 to inhibit the space charge accumulation and as a result show very good sensing performance over a wide pH range (2–12). Ruthenium dioxide sensors have several advantages, compared to both conventional glass pH-electrode and other MOx electrodes[6]:

- higher sensitivity towards hydrogen ions;
- lower sensitivity towards interfering ions;
- faster response;
- longer lifetime;
- smaller hysteresis effect;
- better repeatability;
- lower cost.

RuO_2 electrodes described in the literature are presented in Table 2. The characteristics of the electrodes are discussed in section 1.10. Electrochemical characteristics of the pH-sensitive electrode

1.7.1. Physical and chemical properties of ruthenium dioxide

Ruthenium dioxide (ruthenium (IV) oxide, dioxoruthenium) is an inorganic compound with the molecular formula RuO_2 and a molecular weight of 133.1[21]. Physically it is a blue-black powder with a melting point of 995 °C and a decomposition temperature of 1127 °C[22]. RuO_2 is almost insoluble in water and poorly soluble in acids. It can be reduced to metallic ruthenium by hydrogen or carbon oxide[22].

Table 2. Properties of RuO_2-based electrodes

Electrode sensitive material	Deposition method	Substrate	Precursor	Slope, mV/pH	pH range	Response time, s	T, °C	Hysteresis, mV	Drift, mV/h	Reference electrode	Ref.
RuO_2	ED[3]	Au wire	K_2RuO_4	59.3	2.0 - 12.0	N/A	N/A	N/A	N/A	Normal Hydrogen	Pazstor et al., 1993[23]
		Au disk	$RuCl_3 \cdot xH_2O$	60.5	2.0 – 11.0	7	N/A	N/A	N/A	Ag|AgCl|KCl	Shim et al., 2012[24]
	Screen-printing	Polyester foil	RuO_2-graphite	51.2	2.0 – 10.0	N/A	N/A	N/A	N/A	Saturated calomel	Koncki, Mascini, 1997[25]
			$RuO_2 \cdot xH_2O$	52.1	2.0 – 10.0	15	21-24	N/A	N/A	Ag|AgCl|KCl	Mihell, Atkinson, 1998[26]
			RuO_2	61.8	1.0 – 13.0	14	22	4.6 – 24.9	0.15		Uppuluri et al., 2021[27]
			RuO_2-glass paste	56.0	2.0 – 12.0	120	N/A	N/A	N/A	Screen printed Ag/AgCl	Manjakkal et al., 2016[28]
	MS[4]	Pt wire	RuO_2-glass	60	2.0 – 12.0	90	25	30	3	NHE	McMurray, 1995[29]
		OMC[5]	RuO_2	57.8	2.0 – 12.0	180	22	3.14	19.0	Ag|AgCl|KCl	Lonsdale et al., 2017[30]
		OMC	RuO_2	58.4	4.0 – 10.0	30	22	1.13	5.0		Lonsdale et al., 2017[31]
		Carbon	RuO_2	59.2	4.0 – 10.0	25	22	5.44	20.5		Lonsdale et al., 2017[31]
		Pt	RuO_2	58.6	4.0 – 10.0	20	22	6.45	23.4		Lonsdale et al., 2017[31]
		Pt	RuO_2	56.2	4.0 - 10.0	N/A	37.5	N/A	N/A		Mingels, 2019[32]
		Pt-Ti	RuO_2	59.3	4.0 - 10.0	N/A	37.5	N/A	N/A		Mingels, 2019[32]
		Si	Ru	55.6	1.0 – 13.0	<1	N/A	4.36	0.38		Liao, Chou, 2008[33]
			Ru	51.7	2.0 – 10.0	N/A	N/A	N/A	N/A	SCE	Yao et al., 2020[34]
			RuO_2	55.8	2.0 – 10.0	N/A	N/A	N/A	N/A	SCE	Yao et al., 2020[34]
		Al_2O_3	RuO_2	54-60	2.0 – 10.0	N/A	N/A	N/A	N/A	Ag/AgCl	Kreider et al., 1995[35]
			RuO_2	73.8	4.0 - 10.0	3	22	~ 5	N/A	Ag|AgCl|KCl	Sardarinejad et al., 2015[36]
			RuO_2	58.8	2.0 – 12.0	30	22	1.3	2.9	RuO_2-SiO_2[6]	Lonsdale et al., 2018[19]
			RuO_2	55.7	2.0 – 12.0	30	22	1.66	36	RuO_2-SiO_2	Lonsdale et al., 2019[37]

---

[3] ED – Electrodeposition

[4] MS – Magnetron Sputtering

[5] OMC – Ordered Mesoporous Carbon

[6] RuO_2-SiO_2 – a polyvinylbutyral-SiO_2 modified RuO_2 electrode

Dioxoruthenium crystals have a rutile structure, where the Ru atoms are surrounded octahedrally by six oxide ions, and the O atoms are coordinated by three trigonal planar ruthenium ions (Figure 6). The lattice constant a=449.2 pm and c=310.7 pm (the shortest Ru-Ru distance). The Ru–O distance in the plane where Ru is surrounded by 4 O is 194.2 pm, and in axial O–Ru–O is 198.4 pm[18].

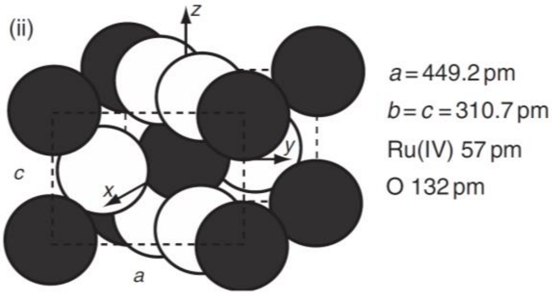

Figure 6. RuO_2 crystals have a rutile structure: black spheres represent ruthenium atoms and white spheres are oxygen atoms (reproduced from[30]).

Ruthenium dioxide powder can be both in crystalline and amorphous state depending on the temperature ruthenium dioxide hydrate powder was dried at. The amorphous powders consist of crystallites with a deformed elementary cell[18]. The amorphous powder has a higher capacitance in comparison with crystalline powder. According to Kurzweil[18], the reason for the higher capacitance of amorphous RuO_2 is its crystalline structure, where water and protons can easily reach RuO_2 adsorption sites, while ordered crystal lattice has too narrow channels.

RuO_2 is a toxic compound with oral lethal doses (LD_{50}) for rats and mice are 4.6 g/kg and 5.6 g/kg of body weight respectively[21]. The toxicity is a very important characteristic of the material, especially when considering the use of the electrode in food samples as some parts of the electrodes material can leak into the sample. Therefore, mixtures of RuO_2 with other MOx is investigated to improve the toxicity of the pH electrode.

1.7.2. Working principle of the ruthenium dioxide pH-electrode

The pH response of the ruthenium dioxide electrode is observed since the surface of the RuO_2 can exchange protons with aqueous solutions[17]. Water molecules bond to the outer layer of ruthenium oxide lattice by the process of dissociative adsorption (Figure 7). Then one hydrogen atom of water molecule bonds to oxygen in ruthenium oxide. As a result, RuO_2 hydrate ($RuO_2 \cdot nH_2O$) is formed as an ordered mixture of Ru-bonded layers of hydroxide and oxide groups. At anodic potentials, protons escape these hydroxide groups and oxide groups are formed. Water serves as a carrier of protons[18]. According to Kurzweil[17], this process is driven by the goal to compensate for the oxygen defect stoichiometry of the lattice. The formation of oxide groups leads to the generation of ruthenium atoms of higher and lower valency, which in turn result in the generation of a potential of the electrode[6].

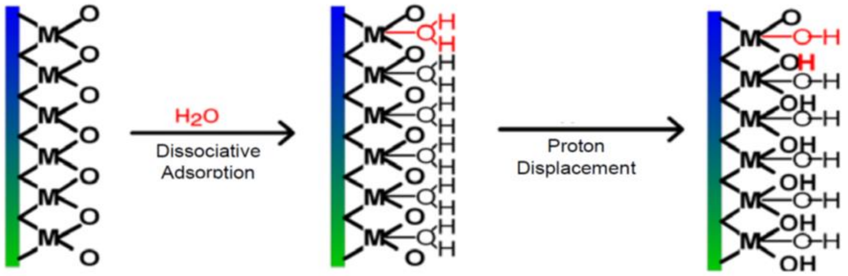

Figure 7. The pH response of the ruthenium dioxide electrode is observed since the surface of the RuO_2 can exchange protons with aqueous solutions. Water molecules bond to the outer layer of ruthenium oxide lattice by the process of dissociative adsorption. Then one hydrogen atom of water molecule bonds to oxygen in ruthenium oxide. As a result, RuO_2 hydrate ($RuO_2 \cdot nH_2O$) is formed (M=[Ru]): $[Ru]+H_2O \rightleftharpoons [Ru]OH_2 \rightleftharpoons [Ru]OH^- + H^+$) (reproduced from [29]).

The mechanism mentioned above can be described by the following equation[17]:

$$\mathrm{RuO_x(OH)_y + ze^- + zH^+ \rightleftharpoons RuO_{x-z}(OH)_{y+z}} \tag{12}$$

Or simplified:

$$\mathrm{Ru^{IV}O_2 + e^- + H^+ \rightleftharpoons Ru^{III}O(OH)} \tag{13}$$

When the RuO_2 electrode is a part of the electrochemical cell, equation (13) describes the half-reaction taking place on the RuO_2 electrode. Quantitatively it can be described by the Nernst equation as follows:

$$\mathrm{E = E^0_{Ru^{IV}/Ru^{III}} - \frac{R \cdot T}{n \cdot F} \cdot \ln \frac{a_{Ru^{III}}}{a_{Ru^{IV}} \cdot a_{H^+}}} \tag{14}$$

As ruthenium oxide is in a solid state, its activity approximates 1 ($a_{Ru(III)}=1$, $a_{Ru(II)}=1$). From equation (13) it can be seen that only one electron participates in the reaction (n=1). Considering this, the Nernst equation (5) for RuO_2 electrode takes the following form (in Volts):

$$E = \mathrm{E^0_{Ru^{IV}/Ru^{III}} - 0.0584 \cdot lg\,[H^+]} \tag{15}$$

Proceeding from the logarithm ($-\mathrm{lg}\, a_{H^+}$) to pH:

$$\mathrm{E = E^0_{Ru^{IV}/Ru^{III}} + 0.0584 \cdot pH} \tag{16}$$

Thus, the pH of an analysed solution can be determined with the use of a RuO_2 electrode by calibrating the electrode in buffers with known pH value and calculating the pH from equation (8). The values $\mathrm{E^0_{Ru^{IV}/Ru^{III}}}$ and the factor before pH (sensitivity) are individual characteristics of an electrode.

1.8. Modified ruthenium dioxide electrodes

1.8.1. Binary metal oxide electrodes

Ruthenium dioxide for the electrode's fabrication can be dopped or mixed with other metal oxides. Such modification can improve the electrocatalytic properties, sensing performance and stability of pH electrodes[38]. Some of the binary materials have also shown better antifouling resistance [39]. Another advantage of the binary oxides is the reduced cost of the electrode's fabrication, as Ruthenium is the most expansive component needed for the electrode's fabrication[40].

In a modified MO_x system, an active transition metal oxide (e.g. RuO_2, IrO_2) is mixed with a chemically inert oxide (e.g. Ta_2O_5, TiO_2)[38]. The MOx can be modified with another oxide in different amounts and therefore 2 types of modified MOx are distinguished: binary oxide electrodes and dopped electrodes. The most common found in literature ratio RuO_2: inert MOx for the binary electrodes is 70:30 mol% respectively. The following binary electrodes with such ratios were investigated in the last years RuO_2-TiO_2[40],[38], RuO_2-Ta_2O_5[41], RuO_2-SnO_2[42]. Furthermore, the electrodes with reverse ratio (30 mol% of RuO_2) for Ta_2O_5[41] and SnO_2[42] were reported. The doped RuO_2 material contains a lower ratio of inert metal oxide. 5 mol% La_2O_3-doped RuO_2[43], 20 mol% Cu_2O-doped RuO_2[44],[39], and $Bi_2Ru_2O_{7+x}$-RuO_2[45] electrodes were described. The sensing properties of the abovementioned electrodes are presented in Table 3.

1.8.2. Modification of RuO_2 electrodes with a Nafion membrane

Another way to modify the metal oxide electrodes is by covering them with a protective layer. Such protection is needed for an electrode when it must be used in samples containing fats and proteins or other common components of food samples. and can adsorb on the electrode's surface[13]. Since the reactions that allow MO_x to sense H^+ ions (e.g., equation (13)) occur on the surface of an electrode, adsorbed fats and proteins can block the measurement. This interruption by fats and proteins is the reason for the limited application of metal-oxide electrodes to the food samples, despite similar to the glass electrodes performance in aqueous media[17],[6]. Coverage of the electrode's pH-sensitive area with a semi-permeable membrane allows to protect the electrode from contamination and overcome this limitation (Figure 8).

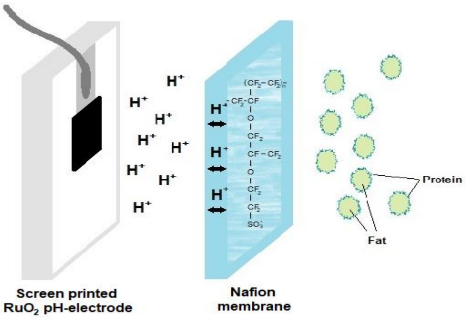

Figure 8. Coverage of the electrode's pH-sensitive area with a semi-permeable Nafion membrane allows protecting the electrode from contamination by fats and proteins present in food samples (reproduced from [13]).

Table 3. Properties of modified RuO_2-based electrodes

Electrode material	**Deposition method**	**Substrate**	**Precursor**	**Slope, mV/pH**	**pH range**	**Response time, s**	**T, ^0C**	**Hysteresis, mV**	**Drift, mV/h**	**Reference electrode**	**Ref.**
RuO_2-Ta_2O_5	Screen-printing	Al_2O_3	RuO_2, Ta_2O_5, glass powder	68.2	2.0 – 12.0	15	N/A	10	N/A	Screen printed Ag/AgCl	Manjakkal et al., 2016[28]
RuO_2-Ta_2O_5			RuO_2, Ta_2O_5	56	2.0 – 12.0	15	N/A	N/A	N/A	Ag|AgCl|KCl	Manjakkal et al., 2016[46]
RuO_2-SnO_2			RuO_2, SnO_2	56.5	2.0 – 12.0	9	N/A	7	N/A		Manjakkal et al., 2015[42]
RuO_2-Cu_2O			RuO_2, Cu_2O	47.4	2.0 – 13.0	N/A	21	N/A	N/A		Zhuiykov et al., 2011[39]
RuO_2-Cu_2O			RuO_2, Cu_2O	N/A	2.0 – 13.0	25	21	N/A	N/A		Zhuiykov et al., 2012[44]
RuO_2-La_2O			RuO_2, La_2O_3	49.3	2.0 – 12.0	N/A	19	N/A	N/A		Zhuiykov et al., 2011[43]
RuO_2-Bi_2O_3			RuO_2, Bi_2O_3	58.0	2.0 – 12.0	~20	23	7	<1		Zhuiykov et al., 2010[45]
RuO_2-Pt			RuO_2	58.0	2.0 – 13.0	1-2	23	~0	1.5		Zhuiykov et al., 2009[47]
RuO_2-TiO_2			RuO_2, TiO_2	56.6	2.0 – 11.0	15	N/A	5	N/A		Manjakkal et al., 2014[48]
RuO_2-TiO_2	Pechini	Ti	$RuCl_3$, Ti	56.0	2.0 – 12.0	N/A	25	N/A	N/A	SCE	Pokrifka et al., 2016 [40]
RuO_2-CNT[7]	Sol-gel	Au, Co, steel	RuO_2, CNT	63.1	2.0 – 12.0	50	N/A	N/A	N/A	SCE	Kahram et al., 2013[49]
RuO_2-CNT	Sputtering	Ta	Ru, CNT	55.5	2.0 – 12.0	40	25	10.2	~3	Ag|AgCl|KCl	Xu, Zhang, 2010[50]
Nafion-modified RuO_2-based electrodes											
RuO_2-Nafion	Screen-printing	Al_2O_3	RuO_2	58.3	2.0 – 12.0	42	22	N/A	0.4	Ag|AgCl|KCl	Uppuluri et al.,2021[27]
			RuO_2-glass paste	58.6	3.0 – 11.0	N/A	N/A	11.5 – 26	N/A		Lazouskaya et al., 2020[51]
RuO_2-Nafion (3 layers)			RuO_2-glass paste	56.5	3.0 – 11.0	N/A	21	10 - 24	25-35		Lazouskaya et al., 2021[13]
RuO_2-Nafion (5 layers)			RuO_2-glass paste	55.1	3.0 – 11.0	N/A	21	20 - 32	25-35		Lazouskaya et al., 2021[13]
RuO_2-Ta_2O_5-Nafion	Sputtering	Al_2O_3	RuO_2	55.3	2.0 – 12.0	136	22	0.7	7.2	RuO_2-SiO_2	Lonsdale, 2018[19]

---

[7] CNT – Carbon Nanotube

One of the materials most extensively used as a filtering membrane in electroanalytical applications is Nafion^{TM} (Nafion) membrane [52]. Nafion is a fluorinated comb-like copolymer with short side chains terminated by sulfonic acid groups (SO^{3-})[53]. A chemical structure of Nafion is presented in Figure 9a. The presence of sulfonic acid side chains in a regular order provides to the compound high proton conductivity of 0.1S/cm[54]. These SO^{3-} groups are organized in clusters that have an approximately spherical shape and resemble inverted micelles. As illustrated in Figure 9b,c. diameter of the cluster is varying between 1.8 and 3.5 nm[53] (according to some sources to 4 nm[54]), with an average of 2.4 nm[53]. These clusters are connected by 1 nm wide channels. The negatively charged sulfonic acid groups that cover the inner side of clusters and channels permit the migration of protons or positive ions[53]. A higher number of water molecules bound in clusters elevates the H^+ ions mobility through the channels in membrane[53].

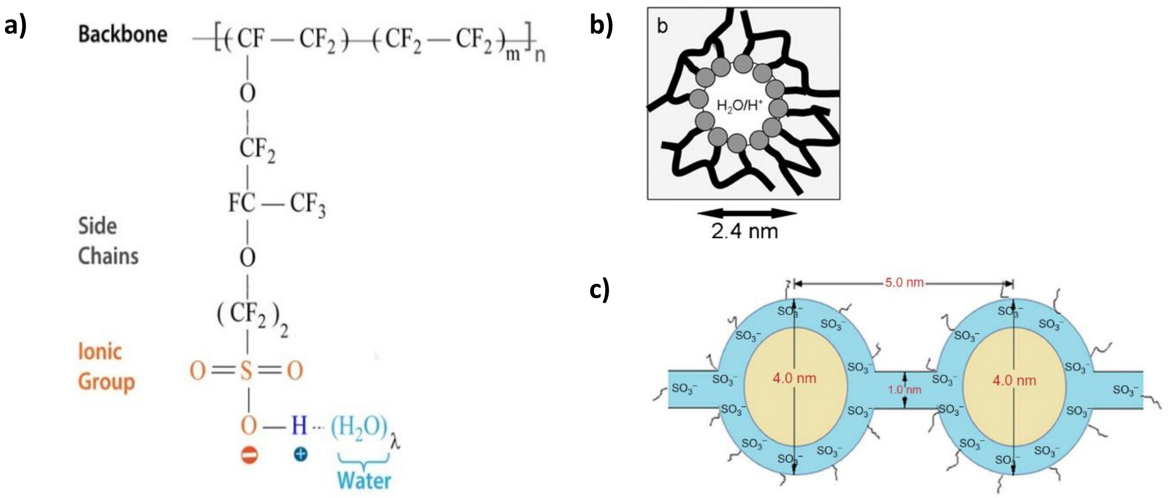

Figure 9. Structure of Nafion: a) Chemical structure of Nafion (adopted from [45]); b) structure of Nafion surrounding water cluster (grey rounds are sulfonic acid groups, black lines are backbone and side chains) (reproduced from [43]) c) model for the structure of inverted-micelle-like water clusters and channels in Nafion (the backbone of Nafion is not shown) (reproduced from [44]).

The Nafion membranes are formed by casting Nafion solution on a suitable substrate and drying at elevated temperatures. The structure of the dried membrane and its properties depend on the distribution of hydrophobic (polymer backbone) and hydrophilic (sulfonic acid groups) parts, which in turn depends on the density and the length of the side chains that may vary in the Nafion structure[53].

Along with the high H^+ ions conductivity, the Nafion membrane has one more important property for pH measurements in food samples: Nafion membrane is resistant to biofouling – the accumulation of proteins, fats, cells, and other biological materials on a surface of the electrode. Biofouling is one of the main reasons for the failure of biosensors for the in vivo application. Nafion membranes at a functional film thickness of approximately 1–2 µm have been successfully used to overcome this problem[55]. Moreover, it was found that the application of Nafion membrane to the sensors prolongs its lifetime more than cellulose membranes[56] showing relatively low adsorption of molecules from solution[55].

Antifouling property and high proton conductivity along with commercial availability and easy application make Nafion a suitable candidate for the protection of RuO_2 electrodes from biological contaminations. The sensing characteristics of Nafion modified RuO_2-electrode are similar to that of unmodified Ruthenium dioxide electrodes (Table 3).

1.9. RuO_2-based electrode's fabrication methods

Several methods were described for the deposition of RuO_2-layer on a substrate. The most employed methods are thermal decomposition[40],[49], magnetron sputtering[35], electrochemical deposition[24],[23], and screen printing[48] (Figure 10). The main advantage of these methods is the possibility to create a very thin film of ruthenium oxide, which makes the fabrication cost-effective.

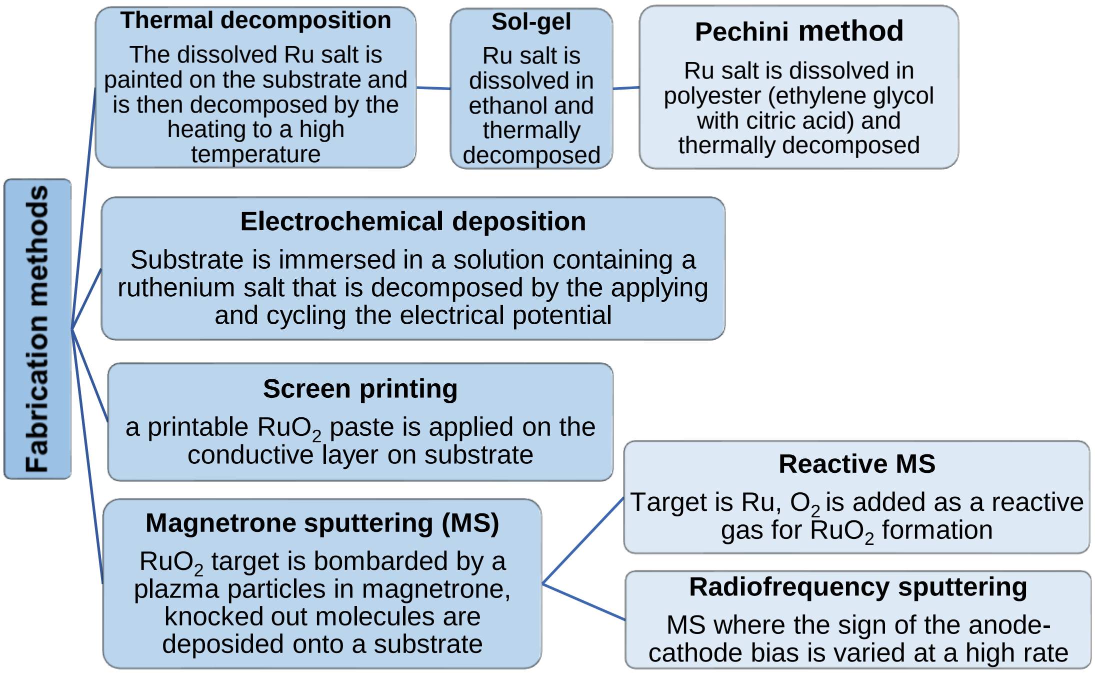

Figure 10. 4 main methods are used for the deposition of RuO_2-layer on a substrate: thermal decomposition, electrochemical deposition, screen printing and magnetrone sputtering.

One of the simplest and cheapest methods of RuO_2 deposition is screen printing[6]. It allows depositing layers with a thickness ranging from a few to a few tens of micrometres[27], that are mechanically strong and well-adhering to different substrates. The technique is based on the deposition of layers of functional materials on a suitable substrate. Each layer is formed from a printable paste by pushing the paste through the screen with a squeegee that moves across the screen (Figure 11). The screen has a stencil that determines the size and shape of the generated layer. Each layer of material undergoes thermal treatment after each printing step.

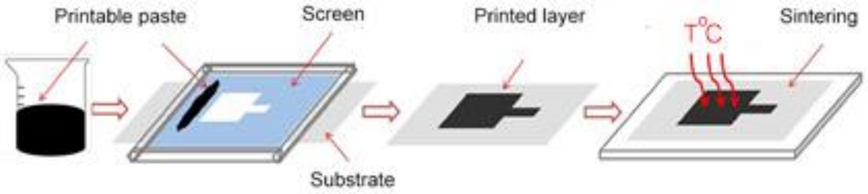

Figure 11. The fabrication of an electrode by the screen printing method is based on the deposition of layers of functional materials on a substrate. Each layer is formed from a printable paste by pushing the paste through the screen. After each printing step, the layer of material undergoes thermal treatment (adopted from [57]).

1.10. Electrochemical characteristics of the pH-sensitive electrode

1.10.1. pH sensitivity

One of the key characteristics of the potentiometric electrode is sensitivity. It allows determining if the electrode works correctly. In the Nernst equation for RuO_2 electrode in the form of equation (16) the factor before pH (0.0584 V/pH or 58.4 mV/pH) is the sensitivity (Nernstian response) for the electrode at room temperature. Theoretically, at temperature 21 °C, the sensitivity value should be 58.4 mV/pH for all the RuO_2-based electrodes (and all pH-sensitive electrodes with n=1). However, in practice deviation from the Nernstian response is observed (Table 2, Table 3). The closer is the sensitivity of the electrode to the theoretical value, the more accurately the electrode works.

1.10.2. The hysteresis effect

The hysteresis effect or the memory effect of an electrode describes how the previous measurement with the electrode influences the next one. The effect is observed when an electrode used repeatedly shows different output voltages for the same buffer solution. According to Liao[33], the hysteresis effect can be regarded as a delay of the pH response. The hysteresis values in the acidic loop are usually smaller than in alkaline. According to Manjakkal et.al.[6], the higher diffusion speed of H^+ ions than OH^- ions can explain this phenomenon.

1.10.3. The potential drift effect

The potential drift effect is the slow non-random change in the reading of an electrode with time in a solution with constant composition, pH and temperature. According to Sardarinejad[58] et al. the drift effect is caused by such dynamic processes as ion neutralization and surface rehydration. This characteristic is important for long-time measurement, which can last for hours, e.g., for control of maturity stage of cheese[59]. The drift effect rate shows if the electrode reading stays stable over a long period of measurement. According to Manjakkal et.al.[6], the drift rate grows with increasing pH value.

1.10.4. Cross-sensitivity

Another important characteristic is cross-sensitivity as samples of water and beverages can contain different salts, sugars, proteins and other components. The cross-sensitivity shows how the presence of different compounds in the sample affects the sensitivity toward H^+ ions of an electrode[27].

1.11. Modern solutions for pH measurement in food products

1.11.1. Types of glass sensors for application in food

Several modifications of a CGE were suggested over the years to overcome the fragility of the glass electrode in the food industry. The most common are commercially available CGEs, covered with stainless steel or plastic (polyvinylidene fluoride (PVDF)) protective bodies. For example, Hanna Instruments (USA) proposes electrodes for different types of food (Figure 12 a-d). The probe for dairy products (Figure 12 a) has a PVDF body and a conical tip with a sleeve type junction, that prevents clogging in viscous liquids such as milk. When the electrode becomes dirty, the sleeve can be moved to clean the glass surface and the junction. Another electrode for dairy products (Figure 12 b) has a PVDF body with a more protected tip and a ceramic outer junction. A penetration style pH electrode presented in Figure 12 c is designed for pH measurements in cheese - with a conical sensing tip, stainless steel sheath and a single junction gel-filled reference. Furthermore, Hanna Instruments has designed a pH probe for meat products (Figure 12 d). The probe comes with a removable stainless steel blade allowing users to make a cut and therefore perform measurements inside the meat sample. The free diffusion junction helps to avoid a clogged reference. All the probes for food products have a built-in temperature sensor. Another solution for pH measurement in meat is proposed by Frontmatec (Denmark). Frontmatec provides a decision for online (Figure 1) monitoring of pH in meat - a glass electrode, covered by a protective steel case with a telescopic sleeve (Figure 12 e).

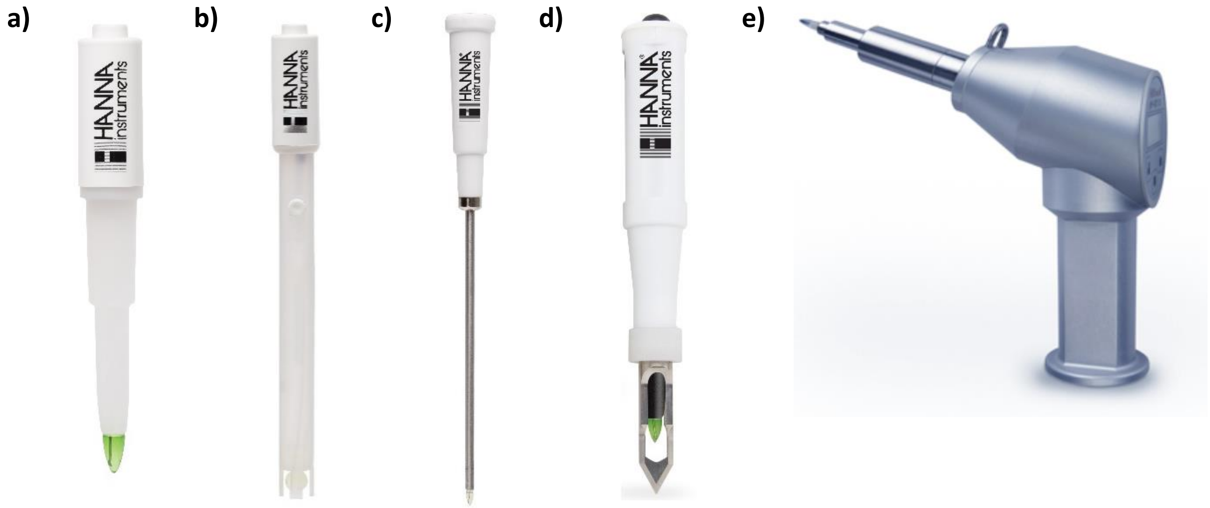

Figure 12. Different types of glass electrodes are presented on the market. The electrodes are designed for specific samples: probes for dairy products have a PVDF body (**a, b**); probe for cheese has stainless steel sheath (**c**); probes for meat can have a stainless-steel blade (reproduced from [60]) or a telescopic steel sleeve (reproduced from [61]) (**e**).

However, the problem of fragility is solved in the abovementioned probes only partially: the electrodes still have sensing glass part, and therefore, can contaminate food, which makes them unusable for inline and online monitoring (Figure 1). At the moment, there are no commercially available glass-free pH electrodes, nevertheless, several novel all-solid-state sensors are reported in the literature. The reported all-solid-state electrodes are discussed in the following section.

1.11.2. Measurements of pH in beverages with solid state electrodes

Huang et al. [62] presented a batteryless radio-frequency transponder with a miniature flexible iridium oxide (IrOx) sensing electrode and silver chloride (AgCl) reference electrode (Figure 13 a). The sol-gel technology (Figure 10) was used for the fabrication of both thin-film electrodes on one polymeric substrate. The system showed a sensitivity of 49.7 mV/pH and was successfully utilised for *in situ* monitoring of the spoilage processes in fish meats continuously for 18 h.

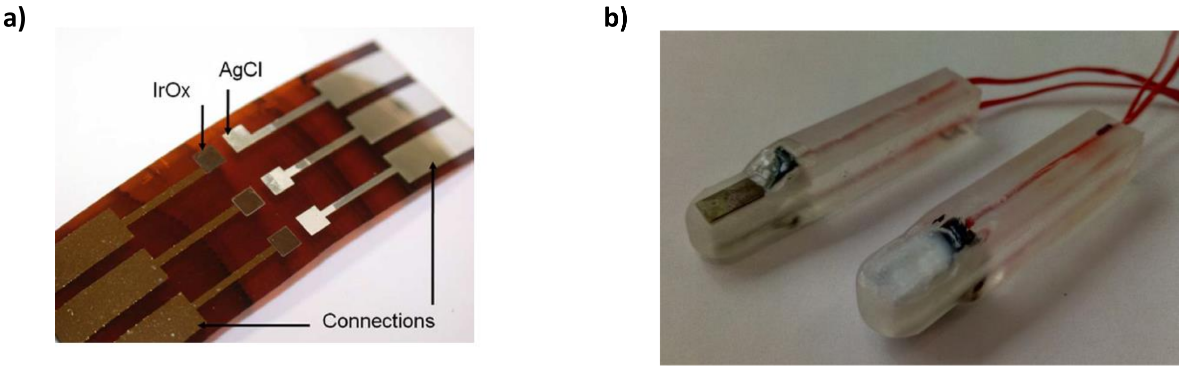

Figure 13. Flexible thin-film IrOx/AgCl sensor for pH measurements in food suggested by Huang et.al. had a sub-Nernstian response (reproduced from [62]) (**a**). Meanwhile, the all-solid-state RuO_2 pH-sensor proposed by Lonsdale et.al. that consisted of an indicator electrode and a polyvinylbutyral-SiO_2 modified RuO_2 reference electrode incorporated in a 3D-printed housing showed close to Nernstian response(reproduced from [37]) (**b**).

Li et.al. [63] developed a sensing systems based on titanium/gold/silver/silver chloride thin-film reference electrode for ion-sensitive field-effect-transistor. Ti, Au and Ag layers were thermally evaporated on a polyethylenenaphthalate substrate. A porous structure polyvinyl butyral membrane was applied on top of the sensor to maintain a constant concentration of chloride. The pH sensitivity of the developed system was 44.8 mV/pH. The measurements in beverages (coca-cola, red bull, orange juice, spring water, etc.) showed good repeatability, however, a significant difference from conventional glass electrode readings was observed.

Lonsdale et al.[37] presented an all-solid-state sensor, that consist of a thin-film sputter-deposited RuO_2 indicator electrode, a polyvinylbutyral-SiO_2 modified RuO_2 reference electrode and 3D-printed electrode housing (Figure 13 b). The fabricated sensor with pH-sensitivity 55.7 mV/pH was applied for pH measurements in different dairy products, including milk with different fat content, cream and yoghurt. The sensor showed good reproducibility (hysteresis < 2 mV) and a moderate level of accuracy (± 0.2 pH).

Furthermore, RuO_2 indicator electrodes were reported by Liao et al.[33] for measurements in beverages, including cola, vinegar and milk. The RuO_2 sensing layer was deposited onto a silicon wafer substrate using radio frequency sputtering technology (Figure 10). The results obtained the pH sensitivity of 55.6 mV/pH and the hysteresis widths ≈4mV. The accuracy for beverage sample measurements did not exceed 5%.

2. Aims of the work

The main objective of this work was to investigate the applicability of RuO_2-based electrodes for pH measurement in beverage samples as an alternative to a conventional glass electrode. Based on this, the main aims of the current thesis were to find answers to the following questions:

1. What are the optimal fabrication conditions for RuO_2-CuO electrodes?
2. Are electrochemical characteristics of the RuO_2-CuO electrodes on par with RuO_2 electrodes and CGE?
3. How does the presence of various ions in the sample affect the result of pH measurement with the studied electrodes?
4. Can binary RuO_2-CuO electrodes outperform the pure RuO_2-electrodes in real water samples?
5. Can binary RuO_2-CuO electrodes outperform the pure RuO_2-electrodes in common beverages?
6. Can the components of beverage samples impact the performance of the fabricated electrodes?
7. What is the most effective way to clean the fabricated electrode after measurements in beverage samples?

3. Materials and methods

3.1. Fabrication of the all-solid-state electrodes

The ruthenium dioxide (RuO_2) and binary ruthenium dioxide-copper oxide (RuO_2-CuO) electrodes were used as received from Łukasiewicz – Krakowski Instytut Technologiczny (Krakow, Poland).

3.1.1. The fabrication of the binary ruthenium dioxide-copper oxide electrodes by screen printing technology

The RuO_2-CuO electrodes were fabricated as previously described by Manjakkal et al.[64] The schematics of the fabrication process is presented in Figure 14. Firstly, an Ag/Pd thick film paste (ESL 9695) was applied on Alumina (Al_2O_3) substrate to create a conductive layer. RuO_2 and CuO were mixed anhydrous in an agate mortar to prepare the paste for the screen printing. Ethylcellulose (analytical grade purity) and terpineol (anhydrous, Fluka Analytical) were used as binders. Mixing was carried out for 20 min to achieve optimal consistency of the paste. The paste was applied to create a sensitive layer that partly overlapping the conductive layer. Each layer was dried at 120 ºC for 15 min and then fired at 850 ºC or 900 ºC for 60 min. Two different temperatures were used to investigate the influence of sintering temperature on the characteristics of the electrode. Following, a copper wire was connected to the conductive layer using Sn/Pb solder. As the final step, a protective layer of silicone rubber (Dow Corning, 3140 RTV) was applied to cover the electrical connection. The sensitive area of the RuO_2-CuO layer that interacts with a sample remained uncovered.

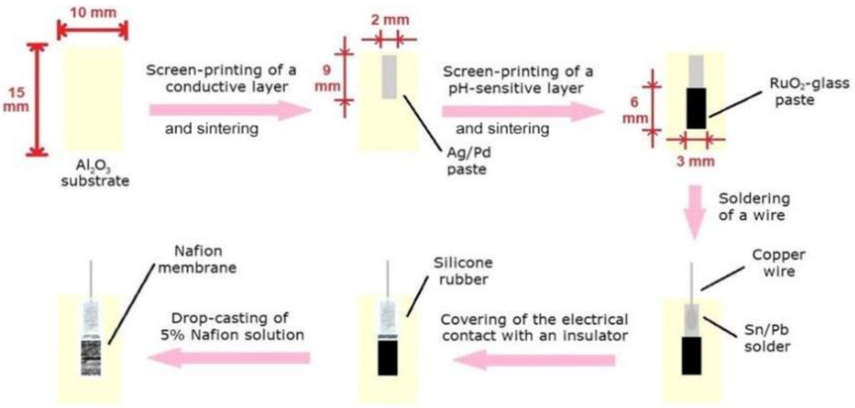

Figure 14. RuO_2-based electrodes were fabricated by screen printing technology as follows: 1 – an Ag/Pd thick film paste is applied on the substrate and sintered, 2 – the RuO_2-CuO paste is applied and sintered, 3 – a copper wire is connected to the conductive layer, 4 – the electrical contact is covered with silicone rubber, 5 – Nafion layer is drop-casted to create a protective layer (reproduced from [24]).

3.1.2. The fabrication of ruthenium dioxide electrodes

The RuO_2 electrodes were fabricated similarly to the RuO_2-CuO electrodes as described in section 3.1.1. The fabrication of the binary ruthenium dioxide-copper oxide electrodes by screen printing technology The only difference was that for the fabrication of the RuO_2 electrodes commercially available ruthenium dioxide paste with the resistivity of 10 kΩ/sq (ESL, 3914) was used. Furthermore, the RuO_2 layer was sintering at 850 ºC as the sintering temperature does not influence the performance of the pure RuO_2 electrodes[27].

3.1.3. Nafion-modification of ruthenium dioxide-based electrodes

The drop-casting technique was used for modification of RuO_2 and RuO_2-CuO electrodes with a Nafion protective layer. The layer was created as previously described by Lazouskaya et al.[51]. Briefly, the sensitive area of the electrode was covered with Nafion by drop-casting of 10 µL of 5% solution of Nafion in a mixture of lower aliphatic alcohols and water (Nafion 117, Sigma Aldrich, USA) (Figure 14). The layer was dried in a laboratory incubator (BD 53, Binder) at 80 °C for 2 hours in between layer deposition. The procedure was repeated 2 more times, therefore, creating 3 layers of Nafion. After the last layer was deposited, the electrodes were left to air-dry at room temperature overnight. The RuO_2 and RuO_2-CuO electrodes, modified with Nafion were named RuO_2-Nf and RuO_2-CuO-Nf respectively.

3.2. Measurement of the characteristics of the potentiometric electrodes

Such electrochemical characteristics as sensitivity, hysteresis and drift effects were determined for 3 types of electrodes: conventional glass electrode, RuO_2-Nf and RuO_2-CuO-Nf. All measurements were carried out in 2 parallel. The cross-sensitivity were measured for Nafion-modified electrodes (RuO_2-Nf and RuO_2-CuO-Nf) as only modified electrodes are being considered for application in beverage samples.

3.2.1. Setup

All the measurements were made by the standard potentiometric method. An electrochemical cell used for this purpose consisted of a fabricated RuO_2, RuO_2-Nafion or RuO_2-CuO-Nafion indicator electrode and a standard glass ion-selective Ag|AgCl|KCl (HI1053P, Hanna Instruments, USA) reference electrode. Both electrodes were connected to the measuring device (Data Acquisition (DAQ) device, USB-6259, National Instruments, USA) through a circuit board with galvanic connections (Figure **15**). The measuring device was powered up by a high-performance digital power supply (E3631A, Agilent, USA) with an input voltage of 12 V. The LabVIEW program (National Instruments, USA) was used to measure the potential difference between the indicator electrode and the reference electrode.

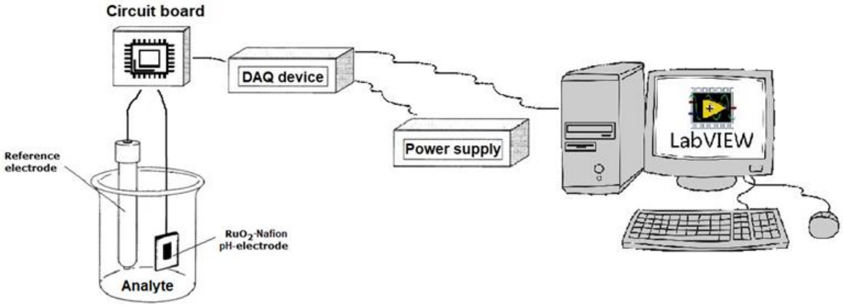

Figure 15. An electrochemical cell for potential measurement consisted of a fabricated RuO_2-based indicator electrode and a standard glass Ag | AgCl | KCl reference electrode, that were connected to the measuring device through a circuit board. The LabVIEW program was used to record results (reproduced from [24]).

3.2.2. pH Sensitivity

The Nernstian equation (16) describes the linear relationship between the electrochemical potential E, and pH value. Hence, for the determination of pH sensitivity of the fabricated RuO_2-based electrodes the electrodes were connected in the potentiometric cell and exposed to buffer solutions of different known pH. The potential of an electrode was registered 90 seconds after immersion of the electrode into a buffer to reach stable potential values. In this study, the E value was measured as a function of pH by a Multifunctional DAQ Device (National Instruments, USA) and the results were recorded using the LabVIEW program. The data were analysed by plotting graph E = f(pH) and calculating the slope of the graph (sensitivity) by the method of least squares (Figure 16).

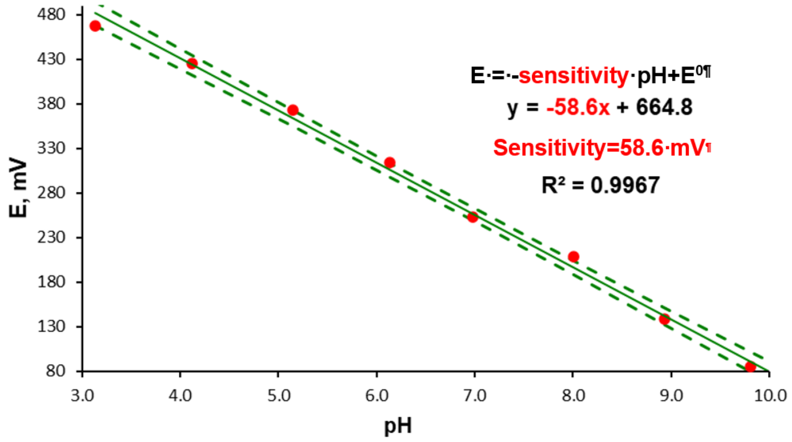

Figure 16. Quantitatively the pH sensitivity of the electrode is the slope of the calibration graph E = f(pH) (green solid line) that is plotted measured electrochemical potential of the electrode exposed to the buffers of different pH. Green dash lines indicate upper and lower confidence limits for α=0.05.

Preparation of Buffer solutions

The buffer solutions of the pH value 3.0 - 11.0 were prepared to evaluate the sensitivity of the fabricated electrodes. The citrate buffers ($(HOC(CO_2H)(CH_2CO_2H)_2 – Na_2HPO_4$) were used for the acidic solutions, phosphate buffers ($NaH_2PO_4 – Na_2HPO_4$) for neutral and slightly basic solutions, and bicarbonate buffer ($Na_2CO_3 – NaHCO_3$) was used for basic solutions. The amounts and types of reagents needed for the preparation of 50 mL of the buffers are indicated in

Table **4**. Salts needed for buffers' preparation were purchased anhydrous from Sigma Aldrich. Fresh buffer solutions were prepared before each measurement and the pH of the solutions was measured with a conventional pH meter (Seven2Go Advanced Single-Channel Portable pH Meter, Mettler Toledo, Switzerland).

Table 4. Reagents used for the preparation of citrate, phosphate, and carbonate buffers

pH	Compound 1	m_1, g	Compound 2	m_2, g
3.0	Citric acid	0.763	Na_2HPO_4	0.292
4.0	Citric acid	0.590	Na_2HPO_4	0.547
5.0	Citric acid	0.466	Na_2HPO_4	0.731
6.0	Citric acid	0.354	Na_2HPO_4	0.897
7.0	NaH_2PO_4	0.234	Na_2HPO_4	0.433
8.0	NaH_2PO_4	0.032	Na_2HPO_4	0.672
9.2	Na_2CO_3	0.053	$NaHCO_3$	0.378
9.9	Na_2CO_3	0.265	$NaHCO_3$	0.210
10.8	Na_2CO_3	0.477	$NaHCO_3$	0.042

3.2.3. The hysteresis effect

The hysteresis effect of the screen printed RuO_2-based electrodes was determined by exposing an electrode to buffer solutions of different pH in a loop manner. Two loops were tested – acidic with pH values 3-5-7-5-3 and alkaline with pH values 11-9-7-9-11. The electrochemical potential of the cell containing the electrode was measured 5 minutes after submersion into each buffer. In between exposures to the different buffers, electrodes were rinsed with Milli-Q water. The hysteresis effect was calculated as the difference of electrode's reading in buffers of the same pH.

3.2.4. The drift effect

The drift effect of the studied electrodes was determined as the difference between the final and initial potential for the measurement for 2 hours in the neutral buffer solution of pH 7 (the buffer prepared as described in section Preparation of Buffer solutions). The drift rate was calculated as the potential difference per one hour by dividing the value of the difference between the final and initial potential by the number of hours of measurement.

3.3. The measurement of cross-sensitivity of fabricated electrodes towards common ions

Cross-sensitivity of RuO_2-Nf and RuO_2-CuO-Nf was measured similarly to sensitivity measurements as described in section 3.2.2. pH SensitivityThe studied compounds were added to the buffers electrodes were exposed to. Added concentration was 0.1M. Used compounds can be divided into 2 groups:

- for measurement of cationic influence – salts with identical anions (chlorides): sodium chloride (NaCl), potassium chloride (KCl), lithium chloride (LiCl), and ammonium chloride (NH_4Cl);
- for measurement of anionic influence – salts with identical cations (sodium): sodium sulphate (Na_2SO_4), sodium L-lactate ($NaC_3H_5O_3$), sodium oxalate ($Na_2C_2O_4$), sodium tartrate ($C_4H_4Na_2O_6$), sodium glutamate ($C_5H_8NO_4Na$), sodium caseinate.

3.4. Evaluation of the performance of the fabricated electrodes in real water samples

3.4.1. Water samples

Four samples of water (Figure 17d) were analysed with the fabricated electrodes. The sea water was collected from Kunda bay of the Baltic Sea near the Toolse castle (Figure 17a) from the surface at a distance of about 3 meters from the shore. The pond water was taken from the surface of the pond (about 15 m in diameter) situated near the sea and forest at Toolse village, Haljala vald, Lääne-Virumaa (Figure 17b). River water samples were collected from a little river that is situated in the same village (Figure 17c) but is not connected to the pond. Tap water was collected from the tap in the TFTAK laboratory in Tallinn. All the samples were collected the day before analysis and stored in the refrigerator. The samples were warmed to room temperature before measurement. pH values of the samples were measured with a conventional pH meter (Seven2Go Advanced Single-Channel Portable pH Meter, Mettler Toledo, Switzerland).

3.4.2. Measurements in real water samples

The pH of water samples from different sources was measured using 2-point calibration. Commercially available certified buffers of pH 4 and 7 (Certipur®, Merk) were used for the calibration. The measurements were made in 5 minutes after immersion into the sample or buffer. pH value was interpolated from the pH values of buffers and measured E values. The electrodes were rinsed with Milli-Q water in between the measurements. All the measurements were made in triplicate.

The performance of the fabricated electrodes was evaluated as the difference of pH values measured with a fabricated electrode and the pH meter (pH difference) on the basis of the following formula:

$$pH\ difference = pH_{fabricated\ electrode} - pH_{pH\ meter} \tag{17}$$

where $pH_{fabricated\ electrode}$ is pH measured with a fabricated electrode and $pH_{pH\ meter}$ is pH value measured with a conventional pH meter.

3.5. Evaluation of the performance of the fabricated electrodes in beverage samples

3.5.1. Samples of caffeinated drinks

5 samples of caffeinated drinks with pH values ranging from 3.2 to 7.3 were used for analysis: coffee (Jacobs' Cronat Gold instant coffee (Jacobs, Germany)) (pH ~5), black tea (Tetley's classic black tea (Tetley, Yorkshire, UK)) (pH ~7-8), green tea (Tetley's classic green tea (Tetley, Yorkshire, UK)) (pH ~6-7), mint tea (Herba's Peppermint Herbal Infusion (Herba, Germany)) (pH ~6-7) and rosehip tea (Herba's Rosehip Herbal Infusion (Herba, Germany)) (pH ~3-4). The coffee granules and tea sachets were purchased from the grocery store, prepared with tap water, and cooled to room temperature (21 °C). pH values of the samples were measured with a conventional pH meter (Seven2Go Advanced Single-Channel Portable pH Meter, Mettler Toledo, Switzerland).

3.5.2. Samples of juices

5 samples of juices with pH values ranging from 2.6 to 4.3 were used for analysis: tomato juice (Aura (A. Le Coq, Estonia)) (pH ~4.3), orange juice (Aura (A. Le Coq, Estonia)) (pH ~4), apple-mango juice (Aura (A. Le Coq, Estonia)) (pH ~4), apple juice (Aura (A. Le Coq, Estonia)) (pH ~3), and lemon juice (Lemon juice concentrate (ICA, Italy)) (pH ~2-3). The juices were purchased from the grocery store. Samples were measured at room temperature (21 °C). pH values of the samples were measured with a conventional pH meter (Seven2Go Advanced Single-Channel Portable pH Meter, Mettler Toledo, Switzerland).

3.5.3. Measurements in beverage samples

The pH of beverage samples was measured similarly to the measurements in real water samples as described in section 3.4.2. Measurements in real water samplesThe measurements in different groups of samples (water, caffeinated drinks and juices) were performed on different days and the calibration was performed at the beginning of each measurement day.

3.6. Measurement of cross-sensitivity of fabricated electrodes towards the components of tomato juice

Cross-sensitivity of RuO_2-Nf and RuO_2-CuO-Nf towards components of tomato juice was measured similarly to cross-sensitivity towards common ions as described in section 3.3. The measurement of cross-sensitivity of fabricated electrodes towards common ions The influence of the presence of the following compounds was studied:

- glucose ($C_6H_{12}O_6$)
- sucrose ($C_{12}H_{22}O_{11}$)
- sodium ascorbate ($C_6H_7NaO_6$).

3.7. Study of the effectiveness of cleaning methods for fabricated electrodes

After pH measurement in food samples, the electrodes need to be cleaned as the food residues can be adsorbed on the surface of the electrode. Four methods of the RuO_2-based electrode's cleaning were studied:

- mechanical cleaning – electrodes were cleaned with a sponge and a dish cleaning liquid, then rinsed with Milli-Q water;
- 0,1 M HCl + mechanically – electrodes were soaked in 0.1M HCl for 10 minutes, and then were cleaned mechanically as described above;
- 1% pepsin in 0.1M HCl – electrodes were soaked in 0.1M HCl with added 1% of pepsin for 10 minutes, and then rinsed with Milli-Q water;
- 0.4 M HCl - electrodes were soaked in 0.4M HCl for 10 minutes and then rinsed with Milli-Q water.

The sensitivity of the electrodes was measured before using them for pH measurement in milk samples and two times after using and cleaning: (i) straight away after cleaning and (ii) after conditioning in Milli-Q water overnight.

Figure 17. The places where water samples were collected: a) Kunda bay of Baltic sea; b) pond in Toolse village; c) river in Toolse village; d) water samples used for RuO_2 electrodes testing.

4. Results and discussion

4.1. The optimal ratio of RuO_2 to CuO for binary electrodes fabrication is 1:1 and optimal sintering temperature is 900 °C

In order to find the optimal ratio of RuO_2 to CuO in the binary electrode composition, two different proportions of RuO_2:CuO were used for electrode fabrication: 1:1 and 2:3 mass % respectively. Moreover, electrodes were sintered at different temperatures of 850°C and 900°C to evaluate the influence of the sintering temperature on the properties of the RuO_2-CuO electrodes. The sensitivity of the fabricated electrodes was measured after one month conditioning in water. Based on the results of the sensitivity measurement (Table 5 and Figure 18), the electrodes with the ratio of RuO_2 to CuO 1:1 and sintering temperature 900°C showed the highest sensitivity towards H^+ ions. Therefore, binary electrodes with RuO_2 to CuO ratio 1:1 sintered at 900°C were selected for further investigation.

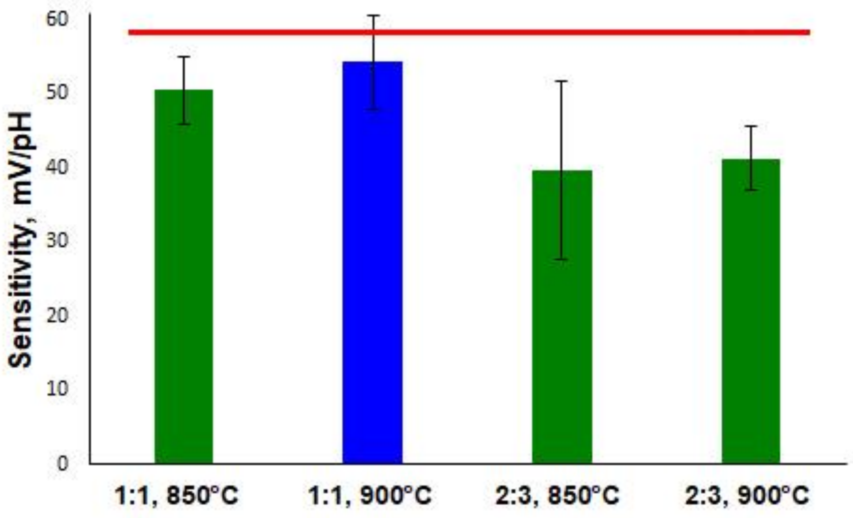

Figure 18. The highest pH sensitivity was observed for binary electrodes with RuO_2:CuO ratio 1:1 sintered at 900°C (blue column), these electrodes were selected for further investigation. pH-sensitivities (Y-axis) of the RuO_2-CuO-Nf electrodes (X-axis) with RuO_2:CuO rate 1:1 and 2:3 and sintering temperature 850 and 900 °C were measured after one-month conditioning in water and compared to Nernstian response (red line).

Table 5. Sensitivity of the RuO_2-CuO-Nf electrodes after one-month conditioning in water.

RuO_2:CuO ratio	**Sintering temperature, °C**	**Sensitivity, mV/pH**	**E^0, mV**	**R^2**
1:1	850	50.5 ± 4.5	554 ± 25.5	0.987
1:1	900	54.3 ± 6.4	587.8 ± 15.6	0.989
2:3	850	39.7 ± 12.0	420.4 ± 148.7	0.959
2:3	900	41.3 ± 4.3	470.0 ± 65.5	0.947

Selected binary electrodes with RuO_2 to CuO ratio 1:1 sintered at 900°C were covered with Nafion as for measurements in beverage samples the electrodes need to be modified. The performance of the bare electrodes (RuO_2 and RuO_2-CuO) and electrodes modified with a Nafion membrane (RuO_2-Nf and RuO_2-CuO-Nf) were compared based on their sensitivity. Furthermore, the electrochemical characteristics of fabricated and modified electrodes were compared to that of a conventional glass electrode.

4.2. Electrochemical characteristics of the fabricated RuO_2-CuO electrodes are comparable to that of RuO_2 electrodes and conventional glass electrode

All the electrodes showed close to the Nernstian response (Figure 19) and characteristics similar to that of CGE (Table 6). Unmodified ruthenium dioxide electrodes showed the sensitivity of 57.5 mV/pH and binary RuO_2-CuO electrodes showed the sensitivity of 54.3 mV/pH, both slightly lower than that of the glass electrode. For Nafion-modified electrodes, a small drop in sensitivity (less than for 1.0 mV/pH) was observed. For both Nafion covered and uncovered electrodes sensitivity of binary RuO_2-CuO electrodes (53.2 and 54.3 mV/pH respectively) was slightly lower than that of RuO_2 electrodes (57.0 and 57.5 mV/pH respectively). Lower sensitivity in the case of CuO-modified RuO_2 electrodes can be attributed to the presence of copper oxide in the pH-sensitive layer of the electrodes. Previously reported by Zaman et al.[58] that the pH sensitivity of the pure CuO electrodes is 28 mV/pH, which is lower than that of RuO_2 electrodes. Therefore, the sensitivity of the RuO_2-CuO electrodes should be somewhat lower than that of the RuO_2 electrodes. The coefficient of determination (R^2) for the Nafion-covered electrodes (0.997 for RuO_2-Nf and 0.990 for RuO_2-CuO-Nf) was slightly higher than that of electrodes without Nafion (0.979 and 0.989 for RuO_2-Nf and RuO_2-CuO-Nf electrodes respectively). Therefore, the introduction of the Nafion membrane does not affect the RuO_2-CuO electrodes performance and Nafion-covered electrodes were investigated further.

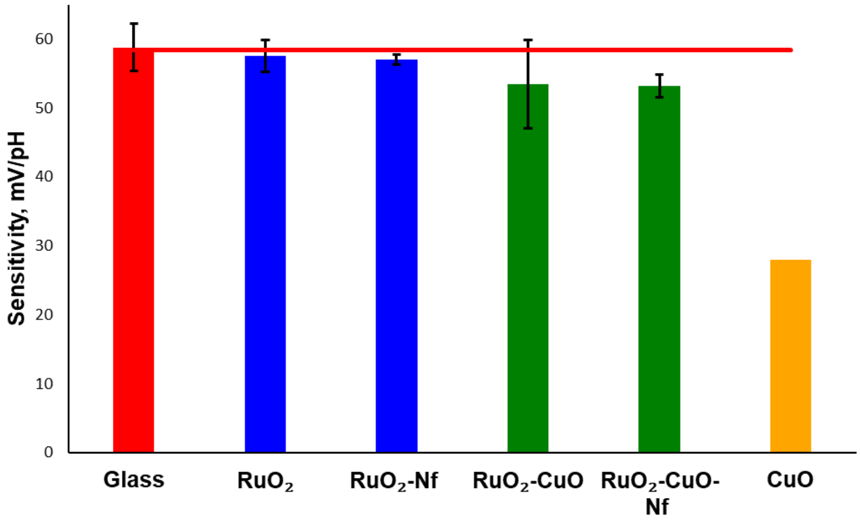

Figure 19. Sensitivity (Y-axis) for the fabricated electrodes (X-axis). RuO_2-CuO and RuO_2-CuO-Nf electrodes (green) showed slightly lower pH sensitivity compared to that of the pure RuO_2 electrodes(blue), glass electrode (red) and the theoretical Nernstian response (red line). Nevertheless, the sensitivity of the RuO_2-CuO and RuO_2-CuO-Nf electrodes was higher than expected taking into account the sensitivity of pure CuO electrodes (orange) (the data on pure CuO electrode is taken from Zaman et al.[58])

Following, the other electrochemical characteristics of the fabricated RuO_2-Nf and RuO_2-CuO-Nf electrodes (hysteresis and drift) were measured and compared to that of a CGE. The results of the measurements are presented in Table 6.

Table 6. Characteristics of fabricated RuO_2-based electrodes

Electrode type	Sensitivity, mV/pH	E^0, mV	R^2	Hysteresis A, mV	Hysteresis B, mV	Drift, mV/h
RuO_2-Nf	57.0 ± 0.7	684.1 ± 2.3	0.997	11 ± 1	17 ± 9	0-15
RuO_2-CuO-Nf	53.2 ± 1.6	575.3 ± 5.5	0.990	5 ± 2	20 ± 3	0-5
Glass electrode						
Glass electrode	58.8 ± 3.4	705.7 ± 36.8	0.997	10 ± 2	12 ± 3	0-5

The hysteresis effect of all the fabricated RuO_2-based electrodes was similar to that of the conventional glass electrode (Table 6) or even smaller (Figure 20 a,b). The electrode of interest RuO_2-CuO-Nf showed the lowest hysteresis value in the acidic loop among all the studied electrodes – 5 mV, but in the basic loop, the hysteresis was the highest of all the measured values – 20 mV. Nevertheless, this value is still acceptable for measurements since it does not exceed even 3.5% of the E^0 value. The low hysteresis values indicate that the measurement is very slightly affected by the previous one and the fabricated electrodes do not need long conditioning in-between measurements in different samples. Smaller hysteresis in the case of the acidic loop can be explained from the point of the size difference of the H^+ and OH^- ions: due to a bigger size, OH^- ions take diffuse, therefore causing increased response time. This phenomenon was also reported previously by Manjakkal et.al.[6].

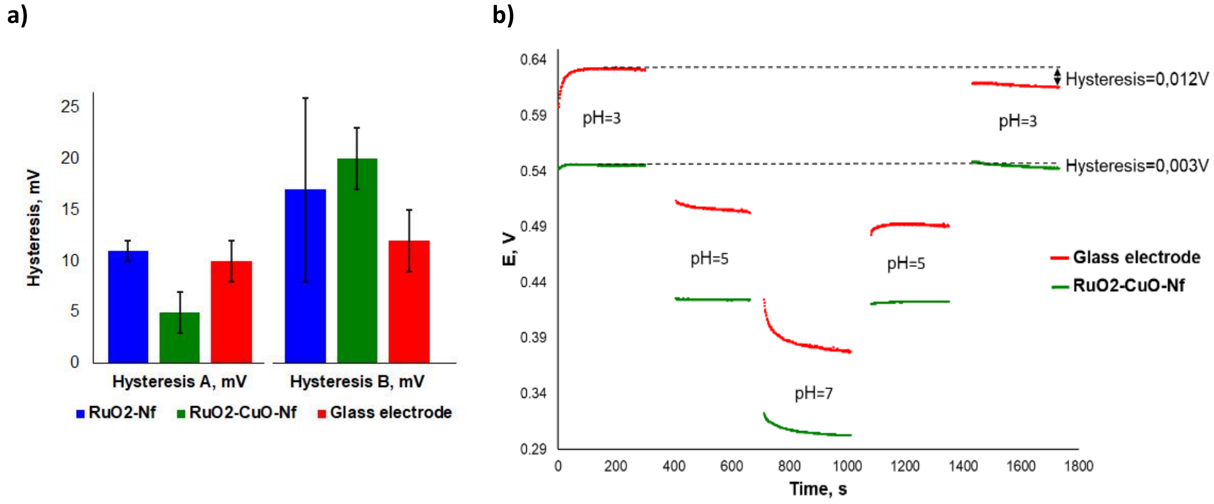

Figure 20. In figure **(a)** the hysteresis values in the acidic loop (Hysteresis A) and the basic loop (Hysteresis B) are presented on the Y-axis for the investigated electrodes: RuO_2-Nf (blue), RuO_2-CuO-Nf (green) and glass electrode (red). Among all the studied electrodes RuO_2-CuO-Nf showed the lowest hysteresis value in the acidic loop (**a,** hysteresis A). Meanwhile, in the basic loop, the hysteresis value was higher yet still acceptable (**a,** hysteresis B**)**, indicating that measurement is very slightly affected by the previous one. In figure **(b)** the change of the electrode's potential (Y-axis) with time (X-axis) is presented. The hysteresis or memory effect is defined as the difference of electrode's reading in buffers of the same pH. The potential response change of electrodes due to hysteresis effect for different solution pH values in the acidic loop (pH 3-5-7-5-3): conventional glass electrode (**b**, red) and RuO_2-CuO-Nf electrode **(b**, green).

All the fabricated electrodes showed an acceptable drift effect (Table 6). The drift effect of the binary RuO_2-CuO-Nf electrodes was similar to that of the CGE 5 mV/h and superior to that of the RuO_2 electrodes (<15 mV/h). Therefore, all the fabricated electrodes can be used for long-time pH measurement. The measured potential drift values correlate well with the data reported by other authors for RuO_2 electrodes. Lonsdale et al.[30] have demonstrated that for RuO_2 electrodes sputtered on different substrates drift values varied from 5 to 23 mV/h for different electrodes. Sardarinejad et al.[30] demonstrated that for their RuO_2 electrodes the drift rate was around 17mV/h.

4.3. The presence of common ions in the sample almost does not affect the result of pH measurement made with ruthenium dioxide-copper oxide electrodes

4.3.1. Fabricated electrodes showed low cross-sensitivity towards cations

In order to study the influence of different cations present in a sample on the performance of the fabricated electrodes, the sensitivity of the fabricated Nafion-modified electrodes was determined in the presence of the following cations: Na^+, K^+, Li^+ and NH_4^+. The cations with the charge +1 were selected for this study since these ions have the same charge as H^+-ion and are the most probable candidates for interfering with electrodes performance.

The pH sensitivity of both fabricated RuO_2-Nf and RuO_2-CuO-Nf electrodes was almost not affected by the presence of studied cations (

Table **7**). The maximum deviation of 3.4 mV/pH was observed for the RuO_2-CuO-Nf electrode. As can be seen from

Figure **21**, the slopes of potential dependency on the pH (the sensitivities of the electrodes) were the same in all the cases. The behaviour of the RuO_2-Nf electrode in the presence of studied cations was very similar to that of the RuO_2-CuO-Nf electrode. For both types of electrodes, the ammonium ion influenced the E^0 value the most, however, the sensitivities of the electrodes were not affected. All the plots have good linearity with the R^2 value higher than 0.995.

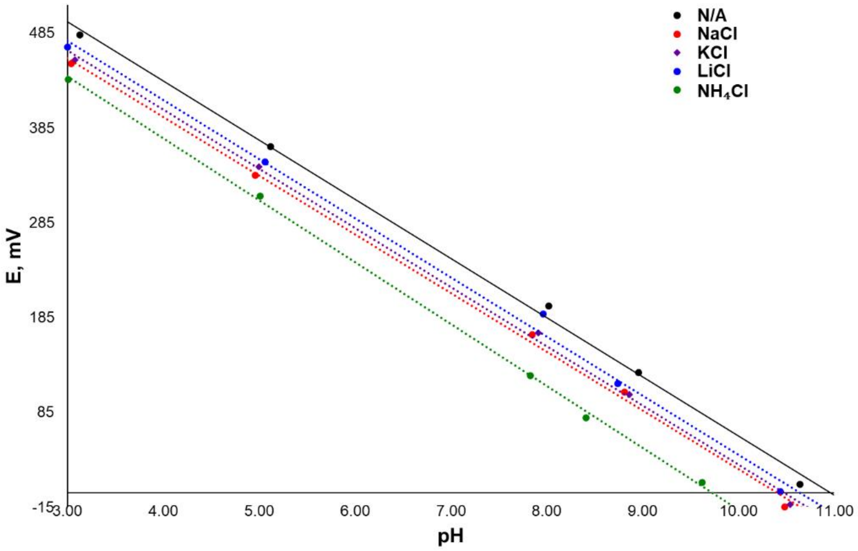

Figure 21. Dependency of the RuO_2-CuO-Nf electrode's potential in buffer solution (Y-axis) on the pH value of the buffer (X-axis) in the presence of the interfering ions: without added salts (black), Na^+ (red), K^+ (purple), Li^+ (blue) and NH_4^+ (green). The pH sensitivity (slope of the calibration plot) of fabricated RuO_2-CuO-Nf electrodes was almost not affected by the presence of studied cations. The calibration plots for RuO_2-CuO-Nf electrode in the presence of Na^+, K^+, Li^+ and NH_4^+ cations are almost parallel to the calibration plot with no ions added. The ammonium ion influenced the E^0 value (the point of intersection of the graph with the Y-axis) the most.

Table 7. Characteristics of the RuO_2-Nf and RuO_2-CuO-Nf electrodes in the presence of the interfering ions

	RuO_2-Nf			**RuO_2-CuO-Nf**		
	Sensitivity, mV/pH	**E^0, mV**	**R^2**	**Sensitivity, mV/pH**	**E^0, mV**	**R^2**
No added salts	59.6	711.2	0.991	62.4	684.1	0.998
NaCl	60.9	699.9	0.998	61.9	644.2	0.998
KCl	61.2	698.9	0.999	62.4	654.4	0.999
LiCl	62.4	707.1	0.999	62.4	664.0	0.995
NH_4Cl	60.1	622.9	0.991	65.3	634.8	0.999
Na_2SO_4	61.5	705.5	1.000	63.8	681.7	0.999
Sodium oxalate	57.7	657.6	0.995	59.6	584.0	0.999
Sodium tartrate	58.7	669.1	0.997	60.4	609.5	0.999
Sodium glutamate	59.3	653.9	0.995	59.2	610.2	0.998
Sodium caseinate	61.3	641.1	0.995	59.4	624.6	0.994

The obtained data is in agreement with results gathered by other researchers for RuO_2-electrodes (Table 2). Uppuluri et al.[27] studied the impact of K^+ and NH_4-cations presence observed the maximum sensitivity decrease by 5 mV/pH for K^+-ions. At the same time, Uppuluri et al. [27] attributed the decreased E^0 values of the RuO_2 electrodes in the presence of $(NH_4)_2SO_4$ to the presence of sulphate ions. However, based on our data, the ammonium ions can influence the performance of the RuO_2 electrodes as well. Manjakkal et al.[6] have shown that Li^+, Na^+, K^+ ions have no big impact on the RuO_2-based electrodes. Furthermore, they have also demonstrated that Cl^- anion do not influence RuO_2-based electrodes performance. This correlates well with the results of our study. For the RuO_2-CuO electrodes, there are no studies on these ions influence on electrodes performance to our knowledge.

4.3.2. Fabricated electrodes showed low cross-sensitivity towards anions

Since the sodium cations do not affect the performance of RuO_2-based electrodes, sodium salts with different anions were used to study the influence of anions on the performance of the fabricated electrodes. The sensitivity was determined in the presence of the following anions: sulphate (SO_4^{2-}), ascorbate ($C_6H_7O_6^-$), oxalate ($C_2O_4^{2-}$), tartrate ($C_4H_4O_6^{2-}$), glutamate ($C_5H_8NO_4^-$), L-lactate ($C_3H_5O_3^-$), caseinate. The results of the measurements are presented in

Table **7**. Both types of fabricated electrodes RuO_2-Nf and RuO_2-CuO-Nf showed low sensitivity to studied anions (

Table 7). The influence of anions was similar to that of cations: the sensitivity of electrodes was almost not affected (Figure 22) while the E^0 values slightly varied. The behaviour of the RuO_2-Nf electrode was once again similar to that of the RuO_2-CuO-Nf electrode.

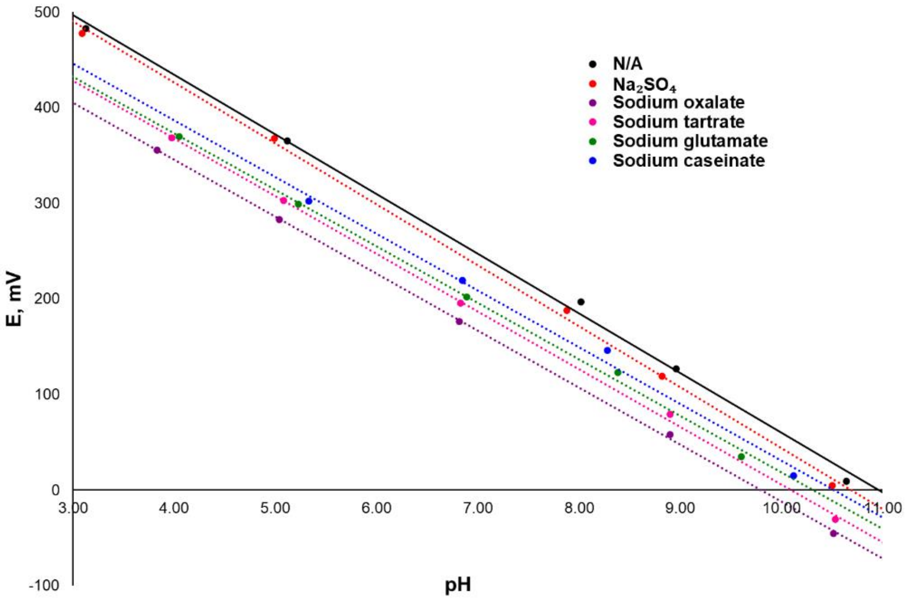

Figure 22. Dependency of the RuO_2-CuO-Nf electrode's potential in buffer solution (Y-axis) on the pH value of the buffer (X-axis) in the presence of the interfering ions: without added salts (black), in the presence of sulphate (red), oxalate (purple), tartrate (pink), glutamate (green) and caseinate (blue). The pH sensitivity (slope of the calibration plot) of fabricated RuO_2-CuO-Nf electrodes was slightly affected by the presence of some studied anions. It is demonstrated by plotting the calibration plots for RuO_2-CuO-Nf electrode in the presence of sulphate oxalate, tartrate, glutamate and caseinate anions next to the plot of the pH sensitivity if the fabricated electrodes when with no ions added to buffer solutions (black). Glutamate and caseinate had the biggest impact on sensitivity. Oxalate influenced the E^0 value (the point of intersection of the graph with the Y-axis) the most.

4.4. The performance of the fabricated ruthenium dioxide-copper oxide electrodes in real water samples was better than that of pure ruthenium electrodes and comparable to the conventional glass electrodes.

Both types of fabricated electrodes RuO_2-Nf and RuO_2-CuO-Nf showed good performance in different water samples (Table 8). In Figure 23 the differences in the pH values measured with the fabricated electrodes and the pH meter are specified on the Oy axis. The average difference for the RuO_2-Nf electrode was 0.23 pH units. RuO_2-CuO-Nf showed even better performance – the average difference was 0.05 pH units.

Table 8. Results of pH measurement with the RuO_2-Nf and RuO_2-CuO-Nf electrodes in water samples.

Sample	pH meter	Glass electrode	RuO_2-Nf	RuO_2-CuO-Nf
Tap water	7.70	7.69 ± 0.02	8.06 ± 0.01	7.68 ± 0.05
Sea water	7.54	7.55 ± 0.02	7.30 ± 0.01	7.50 ± 0.03
River water	7.34	7.35 ± 0.04	7.20 ± 0.05	7.35 ± 0.03
Pond water	7.18	7.17 ± 0.02	6.99 ± 0.05	7.06 ± 0.04

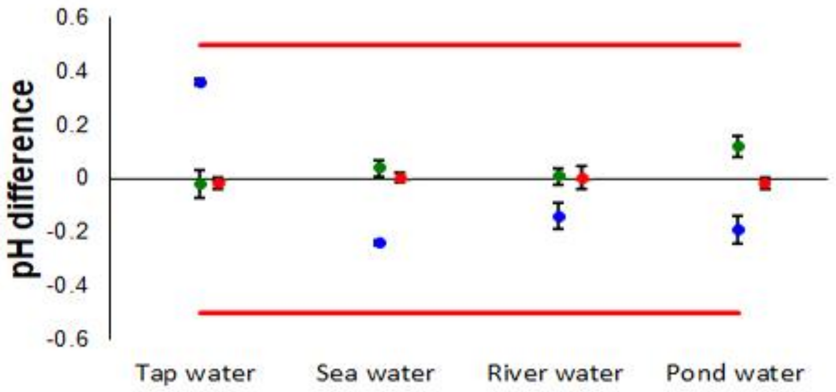

Figure 23. pH values measured with the fabricated electrodes are presented on the Y-axis as a difference of pH values, measured with a studied electrode and pH-meter (pH_{RuO2} - $pH_{pH\text{-}meter}$) for different water samples (X-axis). Blue dots indicate the differences of measurement from pH-meter for RuO_2-Nf electrodes, green dots for RuO_2-CuO-Nf electrodes, red dots for CGE; red lines indicate +0.5pH and -0.5pH difference compared to pH-meter. RuO_2-CuO electrodes showed results closer to those of pH-meter than RuO_2 electrodes.

4.5. The performance of the fabricated binary RuO_2-CuO electrodes in common beverage samples was better than that of pure ruthenium dioxide but poorer than conventional glass electrode

4.5.1. Caffeinated drinks

In caffeinated drinks, fabricated electrodes showed a bigger pH difference compared to the pH meter (Table 9) than in the case of water samples (Table 8). It can be described by the fact that analysed drinks are more complicated matrices than water samples. The average difference in pH for the RuO_2-Nf electrode was 0.54 pH units. The pH of 4 samples of 5 differed from measured with pH-meter by more than 0.5 but less than 0.65 pH units (Figure 24). RuO_2-CuO-Nf electrode showed better performance in caffeinated drinks than RuO_2-Nf electrode. The average pH difference was 0.36 pH units with only one sample pH difference bigger than 0.5 pH units.

Table 9. Results of pH measurement with the RuO_2-Nf and RuO_2-CuO-Nf electrodes in caffeinated drinks samples.

Sample	pH meter	Glass electrode	RuO_2-Nf	RuO_2-CuO-Nf
Black tea	7.31	7.21 ± 0.04	7.95 ± 0.09	7.08 ± 0.09
Green tea	6.97	7.10 ± 0.10	7.56 ± 0.12	6.51 ± 0.20
Mint tea	6.83	6.84 ± 0.02	7.40 ± 0.08	7.05 ± 0.01
Coffee	5.08	5.13 ± 0.01	5.60 ± 0.03	4.74 ± 0.05
Rosehip tea	3.21	3.18 ± 0.01	2.81 ± 0.19	2.66 ± 0.09

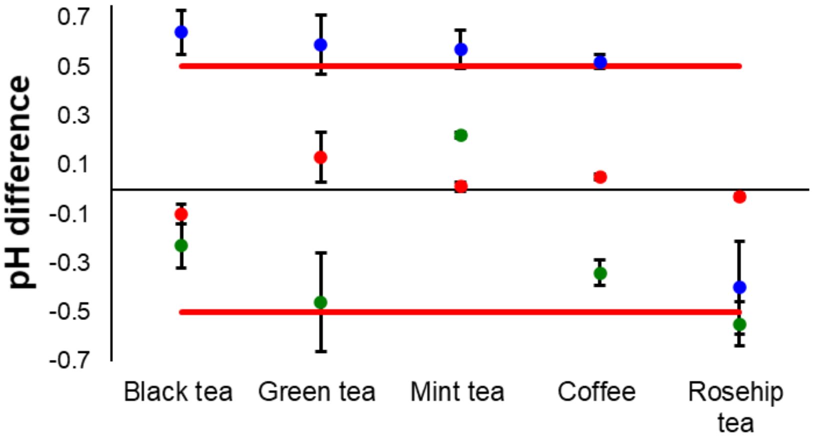

Figure 24. pH values measured with the fabricated electrodes are presented on the Y-axis as a difference of pH values, measured with a studied electrode and pH-meter (pH_{RuO2} - $pH_{pH\text{-}meter}$) for different caffeinated beverages (X-axis). Blue dots indicate the differences of measurement from pH-meter for RuO_2-Nf electrodes, green dots for RuO_2-CuO-Nf electrodes, red dots for CGE; red lines indicate +0.5pH and -0.5pH difference compared to pH-meter. 80% of pH values measured in caffeinated drinks with RuO_2-CuO electrodes and only 20% of values measured with RuO_2 electrodes were in the boundaries of ±0.5pH compared to pH-meter.

4.5.2. Juices

The performance of fabricated electrodes in juice samples was very heterogeneous (Table 10). In apple juice, the pH difference was similar to that of water samples (0.07 pH units for RuO_2-Nf electrode and 0.016 pH units for RuO_2-CuO-Nf electrode). RuO_2-CuO-Nf electrode showed a similar small pH difference in orange juice (0.04 pH units), while for RuO_2-Nf the pH difference in this sample was very big – 1.67 pH units. Both electrodes showed a pH difference of around 0.5 pH units for lemon juice samples (0.66 pH units for RuO_2-Nf electrode and 0.49 pH units for RuO_2-CuO-Nf electrode). In apple-mango and tomato juice samples, the RuO_2-Nf electrode showed a pH difference of 0.73 and 0.4 pH units respectively, while the pH difference for the RuO_2-CuO-Nf electrode was big for these samples – 1.46 and 3.79 pH units respectively. 3 out of 5 measurements in juice samples made with the RuO_2-CuO-Nf electrode and 2 out of 5 measurements made with RuO_2-Nf were in the boundaries ±0.5 pH compared to the pH-meter.

Table 10. Results of pH measurement with the RuO_2-Nf and RuO_2-CuO-Nf electrodes in juice samples

Sample	pH meter	Glass electrode	RuO_2-Nf	RuO_2-CuO-Nf
Lemon juice	2.55	2.44±0.01	3.21±0.09	2.06±0.11
Apple juice	3.06	2.88±0.01	2.99±0.13	2.90±0.08
Apple-mango juice	3.80	3.87±0.01	3.07±0.06	2.34±0.01
Orange juice	3.93	4.04±0.01	3.98±0.19	3.97±0.04
Tomato juice	4.31	4.33±0.01	5.68±0.11	7.00±0.14

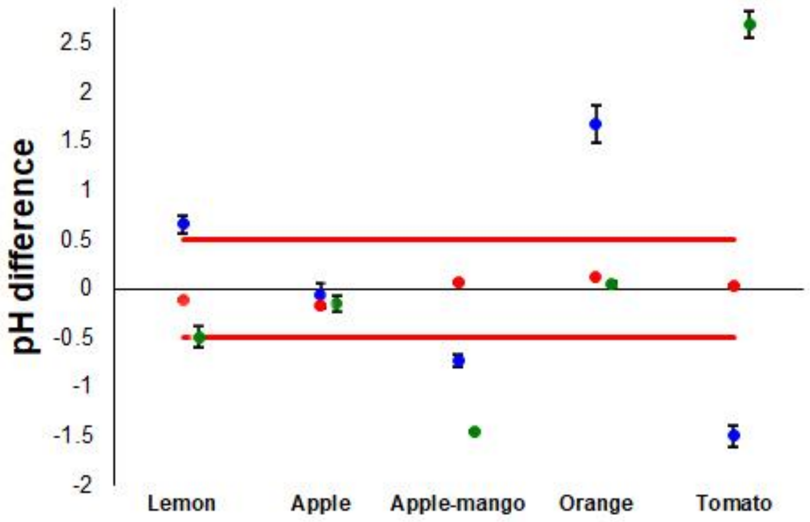

Figure 25. pH values measured with the fabricated electrodes are presented on the Y-axis as a difference of pH values, measured with a studied electrode and pH-meter (pH_{RuO2} - $pH_{pH\text{-}meter}$) for different juices (X-axis). Blue dots indicate the differences of measurement from pH-meter for RuO_2-Nf electrodes, green dots for RuO_2-CuO-Nf electrodes, red dots for CGE; red lines indicate +0.5pH and -0.5pH difference compared to pH-meter. The pH difference measured with RuO_2-CuO electrodes compared to pH-meter in lemon, apple and orange juices was in the boundaries ±0.5pH, while a big error was observed in apple-mango and tomato juices. For the RuO_2 electrodes, the difference exceeded 0.5 pH for orange juice as well.

4.6. Ascorbate ions have a large impact on the pH sensitivity of fabricated electrodes

In order to investigate the reason for the large error of pH measurement in tomato juice, the cross-sensitivity towards some components of this juice was measured (Table 11). It can be seen that sugars almost did not influence characteristics of RuO_2-Nf and RuO_2-CuO-Nf electrodes – similarly to the studied cations and anions the sensitivity change did not exceed 5 and 3 mV/pH respectively, the difference in E^0 value was acceptable as well (Figure 26). The biggest impact on electrode's characteristics had sodium ascorbate: the sensitivity of the RuO_2-CuO-Nf electrode in the presence of ascorbate dropped by 18.2 mV/pH and the sensitivity of RuO_2-Nf was lower by 8.4 mV/pH. The E^0 value dropped for both electrodes drastically- to 182.9 and 184.8 mV respectively.

However, the large error in pH-measurement in tomato juice can not be described only by the presence of ascorbate in the sample, since measurement in lemon and orange juice that is much richer in these ions, showed small error for RuO_2-CuO electrodes (while the error for pure RuO_2 in orange juice was large as well). This phenomenon needs further investigation.

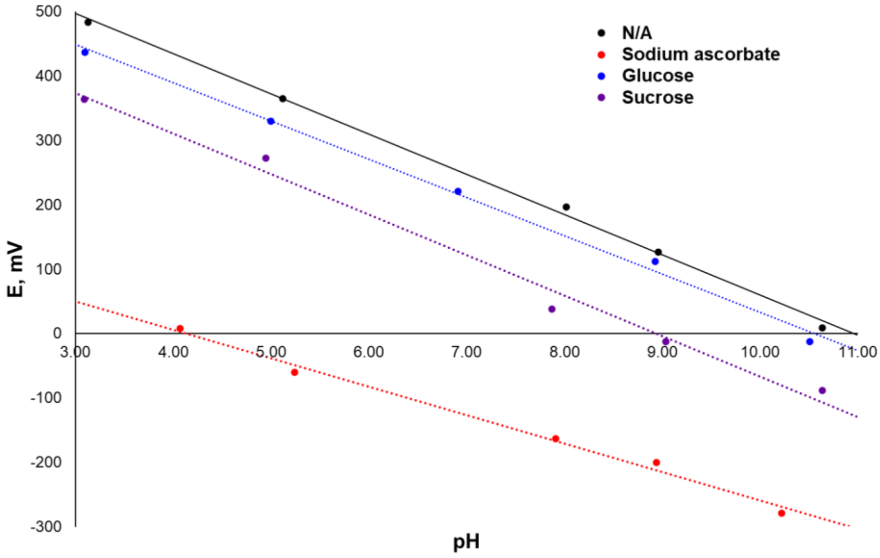

Figure 26. Dependency of the RuO_2-CuO-Nf electrode's potential in buffer solution (Y-axis) on the pH value of the buffer (X-axis) in the presence of the components of the tomato juice: without added compounds (black), in the presence of ascorbate (red), glucose (blue) and sucrose (purple). Both the pH sensitivity and E^0 of the RuO_2-CuO electrode dropped noticeably in the presence of ascorbate ions. Other components did not have such a drastic effect on the sensitivity and E^0.

Table 11. Characteristics of the RuO_2-Nf and RuO_2-CuO-Nf electrodes in the presence of the components of tomato juice.

	RuO_2-Nf			**RuO_2-CuO-Nf**		
	Sensitivity, mV/pH	**E^0, mV**	**R^2**	**Sensitivity, mV/pH**	**E^0, mV**	**R^2**
No added salts	47.3	711.2	0.991	62.4	684.1	0.998
Sodium ascorbate	38.9	184.8	0.990	44.2	182.9	0.992
Glucose	47.2	648.1	0.997	59.4	626.7	0.996
Sucrose	52.2	526.0	0.999	62.8	561.9	0.989

4.7. The combination of soaking in weak acid solution and mechanical treatment is the most effective method for fabricated electrode's cleaning

All the electrodes showed higher sensitivity after cleaning and conditioning (

Table ***12*** and Figure 27). The sensitivities of the electrodes cleaned mechanically both with and without 0.1 M HCl increased after treatment for more than 10.0 mV/pH. After conditioning these electrodes showed the biggest growth in sensitivity – 21.0 and 15.6 mV/pH respectively compared to the untreated electrodes. In the case of cleaning with 1% pepsin in 0.1 M HCl only slight changes in sensitivity were observed – straight away after cleaning it decreased by 1 mV/pH and after conditioning increased by 2.4 mV/pH compared to the initial state. The biggest drop in sensitivity immediately after cleaning was observed for treatment with 0.4 M HCl – 23.2 mv/pH, but after conditioning the sensitivity increased by 12.8 mV/pH.

Considering changes in sensitivity, it can be assumed that mechanical treatment is the most important component of the electrode's cleaning while using it for the pH measurements in food samples, but the combination of mechanical cleaning and the treatment with HCl is the most effective method.

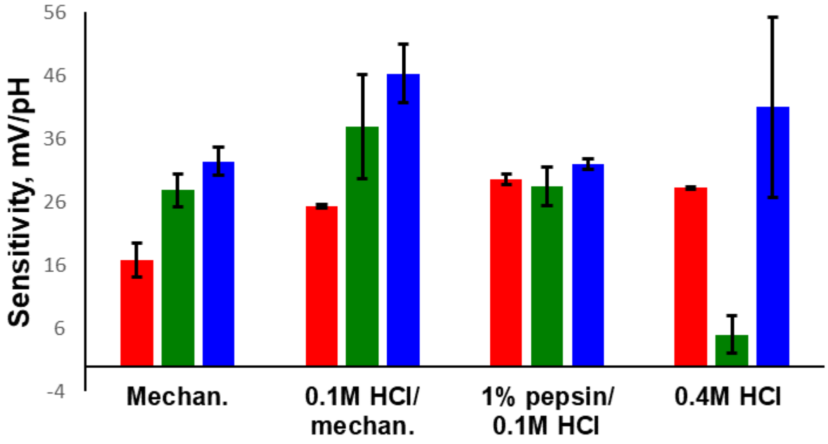

Figure 27. Sensitivity of the RuO_2-Nf electrodes (Y-axis) after different cleaning procedures (X-axis): before cleaning (red), after cleaning (green) and after cleaning and conditioning (blue). The combination of mechanical cleaning and the treatment with HCl was the most effective compared to other methods, proposed in various manuals for cleaning of CGE: mechanical cleaning, cleaning with 1% pepsin and cleaning with 0.4M hydrochloric acid.

Table 12. Characteristics of RuO_2-Nf electrodes before and after cleaning.

	Sensitivity, mV/pH	**E^0, mV**	**R^2**
Mechanically			
Before cleaning	16.8 ± 2.6	484.5 ± 1.5	0.956
After cleaning (straight away)	27.9 ± 2.6	419.0 ± 56.0	0.983
After cleaning (after conditioning)	32.4 ± 2.2	492.0 ± 23.0	0.985
0.1M HCl + mechanically			
Before cleaning	25.3 ± 0.3	523.0 ± 5.0	0.975
After cleaning (straight away)	37.9 ± 8.3	350.5 ± 11.5	0.895
After cleaning (after conditioning)	46.3 ± 4.6	519.5 ± 0.5	0.985
1% pepsin in 0.1M HCl			
Before cleaning	29.6 ± 0.9	561.5 ± 10.5	0.99
After cleaning (straight away)	28.5 ± 3.1	511.5 ± 33.5	0.980
After cleaning (after conditioning)	32.0 ± 0.9	543.5 ± 35.0	0.985
0.4M HCl			
Before cleaning	28.2 ± 0.2	530.5 ± 2.5	0.960
After cleaning (straight away)	5.0 ± 3.0	76.0 ± 90.0	0.265
After cleaning (after conditioning)	41.0 ± 14.2	545.5 ± 89.5	0.965

Abstract

The conventional glass electrode that is currently used for pH measurements in food is mechanically fragile and therefore it can contaminate food with dangerous glass fragments. The all-solid-state proton sensitive ruthenium dioxide electrodes are the modern alternatives to the standard glass electrodes providing improved durability. However, ruthenium is a rare element that is known to be toxic. The partial replacement of ruthenium oxide by the much less toxic and less expensive copper oxide can improve the toxicity and lower the price of the electrode. The binary RuO_2-CuO electrodes were presented in this thesis and their applicability for beverage samples was studied. The electrodes were fabricated by the screen printing method and covered with a Nafion membrane for protection. The best fabrication parameters for the RuO_2-CuO electrodes were determined as 1:1 RuO_2:CuO ratio and sintering temperature of 900°C. The fabricated binary electrodes showed electrochemical characteristics similar to that of pure ruthenium dioxide electrode and conventional glass electrode: the pH-sensitivity of the fabricated electrodes was 53.2 ± 1.6 mV/pH, hysteresis width in the acidic loop was 5mV and in basic – 20 mV, the drift effect did not exceed 5 mV/h. Furthermore, RuO_2-CuO electrodes showed better performance in real-life samples than pure RuO_2 electrodes – the values measured by binary electrodes more often were within the error limits of the pH meter. However, for some juice samples, the error exceeded 0.5 pH, which can be explained by the cross-sensitivity to some of the components of food samples, such as ascorbate ions, that was observed for both RuO_2 and RuO_2-CuO electrodes. Furthermore, the most suitable cleaning procedure for the electrodes was suggested to include mechanical cleaning with soap and consequent cleaning with 0.1M hydrochloric acid.

Considering all the abovementioned, all the 2. Aims of the work were met: electrodes were investigated for their ability to measure pH in real-life samples and compared to the conventional glass electrode. The electrodes were evaluated from the point of their characteristics and applicability for the measurement of pH in real-life samples. Such characteristics as sensitivity, hysteresis, drift effect, and cross-sensitivity were investigated as main electrode characteristics. RuO_2-CuO electrodes exhibited performance similar to that of RuO_2 electrodes and on par with the conventional glass electrode.

The results presented in this work form the basis of research paper that is currently being written with the main supervisor Maryna Lazouskaya as the leading author.

Annotatsioon

pH mõõtmiseks toidus kasutatav standardne klaaselektrood on mehaaniliselt nõrk ja seetõttu võib see saastada toitu ohtlike klaasikildudega. Täiesti tahked (*all-solid-state*) prootonitundlikud ruteeniumdioksiidi elektroodid on kaasaegsed vastupidavamad alternatiivid standardsetele klaaselektroodidele. Ruteenium on haruldane metall, mis on aga teadaolevalt mürgine. Ruteeniumoksiidi osaline asendamine palju vähem toksilise ja odavama vaskoksiidiga võib vähendada sellise elektroodi toksilisust ja alandada elektroodi hinda. Käesolevas lõputöös esitleti binaarseid RuO_2-CuO elektroode ning uuriti nende kasutamist toidus. Elektroodid valmistati siiditrüki (*screen printing*) meetodil ja kaeti kaitseks Nafion membraaniga. Parimad tootmisparameetrid RuO_2-CuO elektroodide jaoks leiti 1:1 RuO_2:CuO suhte korral ja kuumutamistemperatuuril 900°C.

Valmistatud kahekomponentsete elektroodide elektrokeemilised omadused olid sarnased puhta ruteeniumdioksiidi elektroodi ja tavalise klaaselektroodiga: pH-tundlikkus oli 53.2 ± 1.6 mV/pH, hüstereesi laius happelises ahelas oli 5 mV ja aluselises – 20 mV, triiviefekt ei ületanud 5 mV/h. Lisaks näitasid RuO_2-CuO elektroodid tegelikes proovides paremat tööd kui puhtad RuO_2 elektroodid – binaarelektroodidega mõõdetud väärtused jäid sagedamini pH-meetri veapiiridesse. Mõne mahlaproovi puhul ületas viga aga 0.5 pH, mis võib olla seletatav risttundlikkusega mõne toiduproovi komponendi, näiteks askorbaadi ioonide suhtes, mida näitasid nii RuO_2 kui ka RuO_2-CuO elektroodid. Lisaks leiti elektroodide jaoks kõige õigem puhastusprotseduur, mis sisaldas mehaanilist puhastust seebiga ja järgnevat puhastust 0.1M vesinikkloriidhapega.

Kõike eeltoodut arvestades saavutati kõik töö eesmärgid (2. Aims of the work): uuriti elektroodide võimet mõõta pH reaalsetes proovides ja võrreldi tavapärase klaaselektroodiga. Elektroode hinnati nende omaduste ja tegelike proovide pH mõõtmise otstarbekuse seisukohast. Elektroodi peamiste omadustena uuriti selliseid omadusi nagu tundlikkus, hüsterees, triiviefekt ja risttundlikkus. RuO_2-CuO elektroodide töö oli sarnane RuO_2 elektroodidega ja standard klaaselektroodi omaga.

Selles töös esitatud tulemused moodustavad olulise osa hetkel kirjutatavas teadusartiklis, kus juhtivautoriks on juhendaja Maryna Lazouskaya.

Acknowledgements

I would like to thank my supervisors Maryna Lazouskaya and Ott Scheler for giving me the opportunity to make experiments in the Center of Food and Fermentation Technologies (TFTAK). I also would like to thank project Aquasense and TFTAK for providing me with all the necessary materials and equipment.

I would like to express my sincere gratitude to my supervisor Maryna Lazouskaya for her patience, support, and great help throughout the experiments, writing, and editing thesis. Only her guidance and attention to every detail allowed me to write the work in a short time.

Finally, I would like to thank my husband Tõnu and my children Laura and Kristofer for their support and for giving me time to study.

References

[1] "Metrohm. Diagram showing differences between offline, atline, online, and inline analyses." https://metrohm.blog/on-in-at-offline/].

[2] E. R. Cohen *et al.*, "Quantities , Units and Symbols in Physical Chemistry The first and second editions were prepared for publication by," *Int. Union Pure Appl. Chem.*, vol. 233, no. 3, pp. 11–13, 2007.

[3] V. M. Stippl, A. Delgado, and T. M. Becker, "Development of a method for the optical in-situ determination of pH value during high-pressure treatment of fluid food," *Innov. Food Sci. Emerg. Technol.*, vol. 5, no. 3, pp. 285–292, Sep. 2004, doi: 10.1016/J.IFSET.2004.05.002.

[4] A. M. Gibson, N. Bratchell, and T. A. Roberts, "Predicting microbial growth: growth responses of salmonellae in a laboratory medium as affected by pH, sodium chloride and storage temperature," *Int. J. Food Microbiol.*, vol. 6, no. 2, pp. 155–178, Mar. 1988, doi: 10.1016/0168-1605(88)90051-7.

[5] E. Kress-Rogers, "Solid-state pH sensors for food applications," *Trends Food Sci. Technol.*, vol. 2, no. C, pp. 320–324, Jan. 1991, doi: 10.1016/0924-2244(91)90735-2.

[6] L. Manjakkal, D. Szwagierczak, and R. Dahiya, "Metal oxides based electrochemical pH sensors: Current progress and future perspectives," *Prog. Mater. Sci.*, vol. 109, no. February 2019, p. 100635, 2019, doi: 10.1016/j.pmatsci.2019.100635.

[7] D. L. Hopkins, E. N. Ponnampalam, R. J. Van De Ven, and R. D. Warner, "The effect of pH decline rate on the meat and eating quality of beef carcasses," *Anim. Prod. Sci.*, vol. 54, no. 4, pp. 407–413, 2014, doi: 10.1071/AN12314.

[8] K. A. Abbas, A. Mohamed, B. Jamilah, and M. Ebrahimian, "A review on correlations between fish freshness and pH during cold storage," *Am. J. Biochem. Biotechnol.*, vol. 4, no. 4, pp. 416–421, 2008, doi: 10.3844/ajbbsp.2008.416.421.

[9] S. A. Kandeel, A. A. Megahed, M. H. Ebeid, and P. D. Constable, "Ability of milk pH to predict subclinical mastitis and intramammary infection in quarters from lactating dairy cattle," *J. Dairy Sci.*, vol. 102, no. 2, pp. 1417–1427, 2019, doi: 10.3168/jds.2018-14993.

[10] R. Buck *et al.*, "Measurement of pH Definition, Standards, and Procedures," *Handb. Biochem. Mol. Biol. Fourth Ed.*, vol. 74, no. 11, pp. 675–692, 2010, doi: 10.1201/b11923-77.

[11] E. Bakker, *Ion-Selective electrodes | Overview*, 3rd ed. Elsevier Inc., 2019.

[12] I. Dmitrievich, G. Pluglo, O. Fedorova, and A. Komissarenkov, *Elektrokhimicheskiye metody analiza [Electrochemical analysis methods], in Fiziko-khimicheskiye metody analiza [Physical and chemical analysis methods],*. St. Petersburg: Higher School of Technology and Energy, 2014.

[13] M. Lazouskaya, O. Scheler, V. Mikli, K. Uppuluri, K. Zaraska, and M. Tamm, "Nafion Protective Membrane Enables Using Ruthenium Oxide Electrodes for pH Measurement in Milk," *J. Electrochem. Soc.*, vol. 168, no. 10, 2021, [Online]. Available: http://dx.doi.org/10.1149/1945-7111/ac2d3c.

[14] C. Haider, "Monograph Electrodes in Potentiometry," 2004.

[15] "Camlab's blog and information database." https://camblab.info/what-is-the-difference-between-a-single-junction-and-double-junction-ph-electrode/.

[16] "Hanna instruments webpage." https://knowledge.hannainst.com/knowledge/ph-ph-electrodes-what-is-the-difference-between-single-and.

[17] P. Kurzweil, *Metal oxides and ion-exchanging surfaces as pH sensors in liquids: State-of-the-art and outlook*, vol. 9, no. 6. 2009.

[18] P. Kurzweil, "Capacitors | Electrochemical Metal Oxides Capacitors," *Encycl. Electrochem. Power Sources*, no. Ii, pp. 665–678, 2009, doi: 10.1016/B978-044452745-5.00354-3.

[19] W. Lonsdale, M. Wajrak, and K. Alameh, "Manufacture and application of RuO2 solid-state metal-oxide pH sensor to common beverages," *Talanta*, vol. 180, no. December 2017, pp. 277–281, 2018, doi: 10.1016/j.talanta.2017.12.070.

[20] S. Trasatti, "Physical electrochemistry of ceramic oxides," *Electrochim. Acta*, vol. 36, no. 2, pp. 225–241, 1991, doi: 10.1016/0013-4686(91)85244-2.

[21] "National Center for Biotechnology Information. PubChem Compound Summary for CID 82848, Ruthenium(IV) oxide." https://pubchem.ncbi.nlm.nih.gov/compound/82848.

[22] R. Ripan and I. Chetyanu, *Chimiya metallov [Metals chemistry], in Neorganicheskaya chimiya [Inorganic chemistry]*. Moscow: Mir, 1971.

[23] K. Pásztor, A. Sekiguchi, N. Shimo, N. Kitamura, and H. Masuhara, "Electrochemically-deposited RuO2 films as pH sensors," *Sensors Actuators B. Chem.*, vol. 14, no. 1–3, pp. 561–562, 1993, doi: 10.1016/0925-4005(93)85091-N.

[24] J. H. Shim, M. Kang, Y. Lee, and C. Lee, “A nanoporous ruthenium oxide framework for amperometric sensing of glucose and potentiometric sensing of pH,” *Microchim. Acta*, vol. 177, no. 1–2, pp. 211–219, 2012, doi: 10.1007/s00604-012-0774-9.

[25] R. Koncki and M. Mascini, “Screen-printed ruthenium dioxide electrodes for pH measurements,” *Anal. Chim. Acta*, vol. 351, no. 1–3, pp. 143–149, 1997, doi: 10.1016/S0003-2670(97)00367-X.

[26] J. A. Mihell and J. K. Atkinson, “Planar thick-film pH electrodes based on ruthenium dioxide hydrate,” *Sensors Actuators, B Chem.*, vol. 48, no. 1–3, pp. 505–511, 1998, doi: 10.1016/S0925-4005(98)00090-2.

[27] K. Uppuluri, M. Lazouskaya, D. Szwagierczak, K. Zaraska, and M. Tamm, “Fabrication, Potentiometric Characterization, and Application of Screen-Printed RuO 2 pH Electrodes for Water Quality Testing,” *Sensors*, vol. 21, 2021, doi: 10.3390/s21165399.

[28] L. Manjakkal, B. Synkiewicz, K. Zaraska, K. Cvejin, J. Kulawik, and D. Szwagierczak, *Development and characterization of miniaturized LTCC pH sensors with RuO2 based sensing electrodes*, vol. 223. Elsevier B.V., 2016.

[29] H. N. McMurray, P. Douglas, and D. Abbot, “Novel thick-film pH sensors based on ruthenium dioxide-glass composites,” *Sensors Actuators B. Chem.*, vol. 28, no. 1, pp. 9–15, 1995, doi: 10.1016/0925-4005(94)01536-Q.

[30] W. Lonsdale, M. Wajrak, and K. Alameh, “Effect of conditioning protocol, redox species and material thickness on the pH sensitivity and hysteresis of sputtered RuO2 electrodes,” *Sensors Actuators, B Chem.*, vol. 252, pp. 251–256, 2017, doi: 10.1016/j.snb.2017.05.171.

[31] W. Lonsdale, D. K. Maurya, M. Wajrak, and K. Alameh, “Effect of ordered mesoporous carbon contact layer on the sensing performance of sputtered RuO2 thin film pH sensor,” *Talanta*, vol. 164, no. August 2016, pp. 52–56, 2017, doi: 10.1016/j.talanta.2016.11.020.

[32] R. H. G. Mingels, S. Kalsi, Y. Cheong, and H. Morgan, “Iridium and Ruthenium oxide miniature pH sensors: Long-term performance,” *Sensors Actuators, B Chem.*, vol. 297, no. April, p. 126779, 2019, doi: 10.1016/j.snb.2019.126779.

[33] Y. H. Liao and J. C. Chou, “Preparation and characteristics of ruthenium dioxide for pH array sensors with real-time measurement system,” *Sensors Actuators, B Chem.*, vol. 128, no. 2, pp. 603–612, 2008, doi: 10.1016/j.snb.2007.07.023.

[34] X. Yao, M. Vepsäläinen, F. Isa, P. Martin, P. Munroe, and A. Bendavid, “Advanced ruo2 thin films for ph sensing application,” *Sensors (Switzerland)*, vol. 20, no. 22, pp. 1–13, 2020, doi: 10.3390/s20226432.

[35] K. G. Kreider, M. J. Tarlov, and J. P. Cline, “Sputtered thin-film pH electrodes of platinum, palladium, ruthenium, and iridium oxides,” *Sensors Actuators B. Chem.*, vol. 28, no. 3, pp. 167–172, 1995, doi: 10.1016/0925-4005(95)01655-4.

[36] A. Sardarinejad, D. K. Maurya, and K. Alameh, “The pH sensing properties of RF sputtered RuO2 thin-film prepared using different Ar/O2 flow ratio,” *Materials (Basel).*, vol. 8, no. 6, pp. 3352–3363, 2015, doi: 10.3390/ma8063352.

[37] W. Lonsdale, S. P. Shylendra, M. Wajrak, and K. Alameh, “Application of all solid-state 3D printed pH sensor to beverage samples using matrix matched standard,” *Talanta*, vol. 196, no. October 2018, pp. 18–21, 2019, doi: 10.1016/j.talanta.2018.12.037.

[38] L. Manjakkal, “Ph.D. Thesis: Investigation of Potentiometric and Conductimetric Metal Oxide Based pH Sensors Fabricated in Thick Film and LTCC Technology and Their Application in Wireless Monitoring Systems,” Institute of Electron Technology, 2015.

[39] S. Zhuiykov, E. Kats, D. Marney, and K. Kalantar-Zadeh, “Improved antifouling resistance of electrochemical water quality sensors based on Cu2O-doped RuO2 sensing electrode,” *Prog. Org. Coatings*, vol. 70, no. 1, pp. 67–73, 2011, doi: 10.1016/j.porgcoat.2010.10.003.

[40] L. A. Pocrifka, C. Gonçalves, P. Grossi, P. C. Colpa, and E. C. Pereira, “Development of RuO 2-TiO 2 (70-30) mol% for pH measurements,” *Sensors Actuators, B Chem.*, vol. 113, no. 2, pp. 1012–1016, 2006, doi: 10.1016/j.snb.2005.03.087.

[41] L. Manjakkal, K. Zaraska, K. Cvejin, J. Kulawik, and D. Szwagierczak, “Potentiometric RuO2-Ta2O5 pH sensors fabricated using thick film and LTCC technologies,” *Talanta*, vol. 147, pp. 233–240, 2016, doi: 10.1016/j.talanta.2015.09.069.

[42] L. Manjakkal, K. Cvejin, J. Kulawik, K. Zaraska, D. Szwagierczak, and G. Stojanovic, “Sensing mechanism of RuO2-SnO2 thick film pH sensors studied by potentiometric method and electrochemical impedance spectroscopy,” *J. Electroanal. Chem.*, vol. 759, pp. 82–90, 2015, doi: 10.1016/j.jelechem.2015.10.036.

[43] S. Zhuiykov, D. Marney, and E. Kats, “Investigation of electrochemical properties of La2O 3-RuO2 thin-film sensing electrodes used in sensors for the analysis of complex solutions,” *Int. J. Appl. Ceram. Technol.*, vol. 8, no. 5, pp. 1192–1200, 2011, doi: 10.1111/j.1744-7402.2010.02562.x.

[44] S. Zhuiykov, E. Kats, K. Kalantar-Zadeh, M. Breedon, and N. Miura, “Influence of thickness of sub-micron Cu 2O-doped RuO 2 electrode on sensing performance of planar electrochemical pH sensors,” *Mater. Lett.*, vol. 75, pp. 165–168, 2012, doi: 10.1016/j.matlet.2012.01.107.

[45] S. Zhuiykov, “Development of ceramic electrochemical sensor based on Bi2Ru2O7+x-RuO2 sub-micron oxide sensing electrode for water quality monitoring,” *Ceram. Int.*, vol. 36, pp. 2407-2413., 2010.

[46] L. Manjakkal, K. Cvejin, J. Kulawik, K. Zaraska, R. P. Socha, and D. Szwagierczak, “X-ray photoelectron spectroscopic and electrochemical impedance spectroscopic analysis of RuO2-Ta2O5 thick film pH sensors,” *Anal. Chim. Acta*, vol. 931, pp. 47–56, 2016, doi: 10.1016/j.aca.2016.05.012.

[47] S. Zhuiykov, “Morphology of Pt-doped nanofabricated RuO2 sensing electrodes and their properties in water quality monitoring sensors,” *Sensors Actuators, B Chem.*, vol. 136, no. 1, pp. 248–256, 2009, doi: 10.1016/j.snb.2008.10.030.

[48] L. Manjakkal, K. Cvejin, J. Kulawik, K. Zaraska, D. Szwagierczak, and R. P. Socha, “Fabrication of thick film sensitive RuO2-TiO2 and Ag/AgCl/KCl reference electrodes and their application for pH measurements,” *Sensors Actuators, B Chem.*, vol. 204, pp. 57–67, 2014, doi: 10.1016/j.snb.2014.07.067.

[49] M. Kahram, M. Asnavandi, and A. Dolati, “Synthesis and electrochemical characterization of sol-gel-derived RuO 2/carbon nanotube composites,” *J. Solid State Electrochem.*, vol. 18, no. 4, pp. 993–1003, 2014, doi: 10.1007/s10008-013-2346-2.

[50] B. Xu and W. De Zhang, “Modification of vertically aligned carbon nanotubes with RuO2 for a solid-state pH sensor,” *Electrochim. Acta*, vol. 55, no. 8, pp. 2859–2864, 2010, doi: 10.1016/j.electacta.2009.12.099.

[51] M. Lazouskaya, M. Tamm, O. Scheler, K. Uppuluri, and K. Zaraska, “Nafion as a protective membrane for screen-printed pH-sensitive ruthenium oxide electrodes,” *Proc. Bienn. Balt. Electron. Conf. BEC*, vol. 2020-Octob, 2020, doi: 10.1109/BEC49624.2020.9276822.

[52] E. Leppänen, A. Peltonen, J. Seitsonen, J. Koskinen, and T. Laurila, “Effect of thickness and additional elements on the filtering properties of a thin Nafion layer,” *J. Electroanal. Chem.*, vol. 843, no. February, pp. 12–21, 2019, doi: 10.1016/j.jelechem.2019.05.002.

[53] R. Hiesgen, E. Aleksandrova, G. Meichsner, I. Wehl, E. Roduner, and K. A. Friedrich, “High-resolution imaging of ion conductivity of Nafion® membranes with electrochemical atomic force microscopy,” *Electrochim. Acta*, vol. 55, no. 2, pp. 423–429, 2009, doi: 10.1016/j.electacta.2009.05.049.

[54] P. Kumar, R. P. Bharti, V. Kumar, and P. P. Kundu, *Polymer electrolyte membranes for microbial fuel cells: Part a. nafion-based membranes*. Elsevier B.V., 2018.

[55] N. Wisniewski and M. Reichert, “Methods for reducing biosensor membrane biofouling,” *Colloids Surfaces B Biointerfaces*, vol. 18, pp. 197–219, 2000.

[56] D. J. Harrison, R. F. B. Turner, and H. P. Baltes, “Characterization of Perfluorosulfonic Acid Polymer Coated Enzyme Electrodes and a Miniaturized Integrated Potentiostat for Glucose Analysis in Whole Blood,” *Anal. Chem.*, vol. 60, no. 19, pp. 2002–2007, 1988, doi: 10.1021/ac00170a003.

[57] X. Xu, M. Luo, P. He, X. Guo, and J. Yang, “Screen printed graphene electrodes on textile for wearable electrocardiogram monitoring,” *Appl. Phys. A Mater. Sci. Process.*, vol. 125, no. 10, pp. 1–7, 2019, doi: 10.1007/s00339-019-3006-x.

[58] S. Zaman, M. H. Asif, A. Zainelabdin, G. Amin, O. Nur, and M. Willander, “CuO nanoflowers as an electrochemical pH sensor and the effect of pH on the growth,” *J. Electroanal. Chem.*, vol. 662, no. 2, pp. 421–425, 2011, doi: 10.1016/j.jelechem.2011.09.015.

[59] C. Phadungath, “The mechanism and properties of acid-coagulated milk gels,” *Songklanakarin J. Sci. Technol.*, vol. 27, no. 2, pp. 433–448, 2005.

[60] “Hanna Instruments web page.” https://hannainst.lt/en/produkto-kategorija/ph-ir-ph-orp-matuokliai/.

[61] “Frontmatec Web Page.” https://www.frontmatec.com/en/other/instruments/quality-control/ph-k21.

[62] W. D. Huang, S. Deb, Y. S. Seo, S. Rao, M. Chiao, and J. C. Chiao, “A passive radio-frequency pH-Sensing tag for wireless food-quality monitoring,” *IEEE Sens. J.*, vol. 12, no. 3, pp. 487–495, 2012, doi: 10.1109/JSEN.2011.2107738.

[63] Q. Li *et al.*, “Stable thin-film reference electrode on plastic substrate for all-solid-state ion-sensitive field-effect transistor sensing system,” *IEEE Electron Device Lett.*, vol. 38, no. 10, pp. 1469–1472, 2017, doi: 10.1109/LED.2017.2732352.

[64] L. Manjakkal, K. Cvejin, J. Kulavik, K. Zaraska, and D. Szwagierczak, “The effect of sheet resistivity and storage conditions on sensitivity of Ruo2 based pH sensors,” *Key Eng. Mater.*, vol. 605, pp. 457–460, 2014, doi: 10.4028/www.scientific.net/KEM.605.457.